AD-A137 711 ON QUANTIFYING THE SIMILARITIES OF PROPAGATION LOSS CURVES(U) PLANNING SYSTEMS INC MCLEAN VA A E BARNES 15 JAN 80 PSI-TR-127119 N00014-79-C-0695 1/1

UNCLASSIFIED F/G 12/1 NL

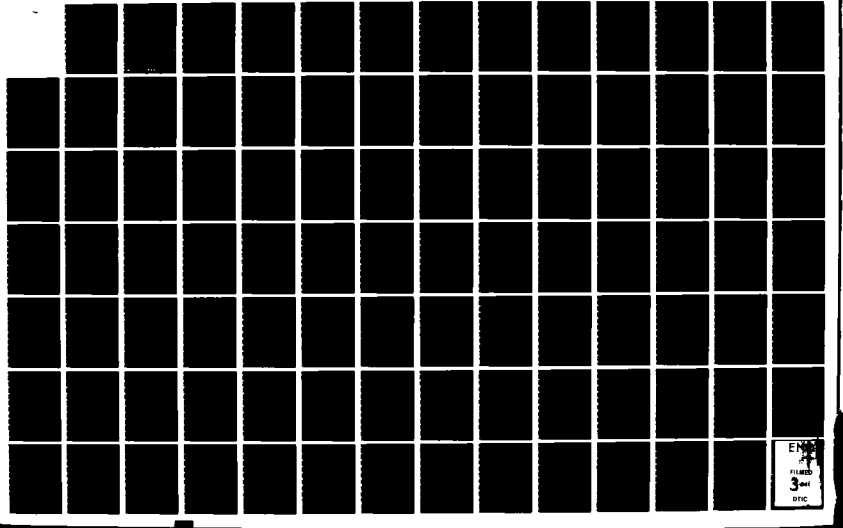

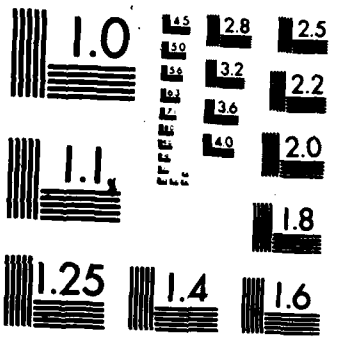

# ON QUANTIFYING THE SIMILARITIES OF PROPAGATION LOSS CURVES

Allen E. Barnes

15 January 1980

PSI Technical Note
TR-127119

Prepared for:

Naval Ocean Research and Development Activity
Code 321
NSTL Station, Mississippi 39529



Prepared by:

Planning Systems Incorporated
7900 Westpark Drive
McLean, Virginia 22102

SECURITY CLASSIFICATION OF THIS PAGE *(When Data Entered)*

| REPORT DOCUMENTATION PAGE | | READ INSTRUCTIONS BEFORE COMPLETING FORM |
|---|---|---|
| 1. REPORT NUMBER<br>PSI-TR-127119 | 2. GOVT ACCESSION NO.<br>AD-A137 711 | 3. RECIPIENT'S CATALOG NUMBER |
| 4. TITLE *(and Subtitle)*<br>ON QUANTIFYING THE SIMILARITIES OF PROPAGATION LOSS CURVES | | 5. TYPE OF REPORT & PERIOD COVERED<br>FINAL<br>6. PERFORMING ORG. REPORT NUMBER<br>PSI-TR-127119 |
| 7. AUTHOR(s)<br>ALLEN E. BARNES | | 8. CONTRACT OR GRANT NUMBER(s)<br>N00014-79-C-0695 |
| 9. PERFORMING ORGANIZATION NAME AND ADDRESS<br>PLANNING SYSTEMS, INC.<br>7900 WESTPARK DRIVE<br>MCLEAN, VA 22102 | | 10. PROGRAM ELEMENT, PROJECT, TASK AREA & WORK UNIT NUMBERS<br>63708N |
| 11. CONTROLLING OFFICE NAME AND ADDRESS<br>NAVLA OCEAN RESEARCH AND DEVELOPMENT ACTIVITY<br>CODE 323<br>NSTL STATION, MS 39529 | | 12. REPORT DATE<br>15 JAN 1980<br>13. NUMBER OF PAGES<br>73 |
| 14. MONITORING AGENCY NAME & ADDRESS*(if different from Controlling Office)* | | 15. SECURITY CLASS. *(of this report)*<br>UNCLASSIFIED<br>15a. DECLASSIFICATION/DOWNGRADING SCHEDULE |

16. DISTRIBUTION STATEMENT *(of this Report)*

APPROVED FOR PUBLIC RELEASE: DISTRIBUTION UNLIMITED

17. DISTRIBUTION STATEMENT *(of the abstract entered in Block 20, if different from Report)*

18. SUPPLEMENTARY NOTES

19. KEY WORDS *(Continue on reverse side if necessary and identify by block number)*

PROPAGATION LOSS; MODEL EVALUATION; QUANTITATIVE COMPARISON

20. ABSTRACT *(Continue on reverse side if necessary and identify by block number)*

A series of measures are developed which may be applied to transmission loss curves to quantitatively describe them and afford a quantitative means of comparison.



DD FORM 1 JAN 73 1473 EDITION OF 1 NOV 65 IS OBSOLETE
S/N 0102-LF-014-6601

SECURITY CLASSIFICATION OF THIS PAGE *(When Data Entered)*

TABLE OF CONTENTS

## I. Introduction

Intuitively, if one has two sets of environmental data which are "close," and one uses them as inputs to a transmission loss model, then one would expect the resulting transmission loss curves to be "close." Furthermore, if two sets of environmental data have little or nothing in common, one is not surprised if their resulting transmission loss curves vary greatly. From this rather modest hypothesis, one can develop some sort of mental "scale" which qualitatively compares transmission loss curves. Such a scale could have values such as "seems close," "looks entirely different," and any number of other shades of grading. Yet, such a concept, often based on visual inspection, is still very subjective.

If one is going to seriously consider the U.S. Navy's ability to predict transmission loss, then it is inadequate to merely address the models: transmission loss models currently exist which are quite sophisticated. One must also consider the variability (or, in some cases, the accuracy) of the environmental inputs. The link between environmental changes and transmission loss changes is the model itself. If one is to analytically approach questions dealing with similarities or differences in transmission loss curves produced from different input, it is necessary to establish quantitative measures on the transmission loss curves: "close" is not good enough. The purpose of this paper is to develop a series of measures which may be applied to transmission loss curves to quantitatively describe them and afford a quantitative means of comparison.

It should be noted at the outset, however, that the intuitive statement opening this report is not always true. A small change in the environment can dramatically alter the transmission loss at a point ( cf. Ch. II) by shifting a caustic. And, if the sound speed is altered so that the change in the profile $c(z)$ is small, but the change in the derivative with respect to depth, $\partial c/\partial z$, is large,

then the transmission loss field can be very different. But "in general," one will observe that a small change in the input usually results in a small change in the transmission loss curve.

In regard to our approach, one would think that a metric[1] to measure "closeness" of two transmission loss curves could be devised, i.e., given any two transmission loss curves, one could plug them into a formula and come up with a single number. This is indeed true, but what meaning would it have? Consider a transmission loss curve which is basically 10 log r loss, with prominent convergence zones. Does one say that this curve is "closer" to an 18 log r loss curve with the same prominent convergence zones than it is to a monotonic 10 log r loss curve with no convergence zones? One is essentially comparing apples and oranges, and it is felt that such metrics tend to confuse rather than enlighten. Thus, we have developed a series of measures describing various characteristics of the curves.

## II. Statement of Problem

Given two[2] transmission loss curves (i.e., TL in dB re some standard versus range in some units), define some quantitative measures to indicate the similarity or difference of the curves. These measures must be such that a computer may obtain them, and do so in a reasonably time-efficient manner.[3]

The approach of looking at transmission loss verses range means that curves of the same environmental parameters, but differing receiver depths, may be compared. But, it precludes the direct comparison of an entire transmission loss field (i.e., a grid of TL at various ranges and depths) with another transmission loss field.[4]

Further difficulties arise through the mode of describing the transmission loss curves. For although the curves theoretically extend over all positive reals, in actuality one does not measure transmission loss to an infinite distance nor to an infinitesimal

---

[1] Since footnotes have an occasional but unfortunate habit of being lengthy, they have all been relegated to a section in the rear, following the appendices. Note 1 will be found there.

distance. Thus, the curve whose domain is $(0, \infty)$, is actually specified on a closed subset of this open interval. Furthermore, whether the transmission loss is measured or calculated, it is represented not by a curve, but by a discrete set of points. When one compares two transmission loss "curves" in a computer, one is actually dealing with two sets of discrete points, and their grids may be completely different. This implies that simple expressions such as the difference of two transmission loss curves

$$T_1(r) - T_2(r)$$

may not be directly computable from the data. It will always be assumed, however, that we are working with transmission loss curves, not points, as curves may be constructed by interpolation between the points.[5]

Now that the problem has been stated, along with a few relevant observations, one may briefly consider the classical approach. Let $T_1(r)$ and $T_2(r)$ be two transmission loss functions, and assume that the closed interval [a, b] is within the domain of each function.[6]. For any $p \geq 1$, we may consider the $L_p$ norm of the differences, i.e.

$$\|T_1 - T_2\|_p \equiv L_p(T_1-T_2) \stackrel{d}{=} \left\{\frac{1}{b-a}\int_a^b |T_1(r)-T_2(r)|^p dr\right\}^{1/p}$$

The three common $L_p$ norms are

$\|T_1 - T_2\|_1$ = Average difference between the curves

$\|T_1 - T_2\|_2$ = Root-Mean-Square deviation of curves

$\|T_1 - T_2\|_\infty$ = Maximum difference between

These measures, for $p>1$, are quite handy and are often used[7], but they do not provide an adequate measure for the situation where the transmission loss curves differ by the horizontal shift of a

convergence zone. Suppose the curve $T_1$ has a caustic followed by a shadow zone, with a drop of say 30 dB. If a slightly different environment is used, a new curve, $T_2$ may be produced which is similar, buth with a slight horizontal shift[8] (Fig. 1). Then, although the $L_1$ norm is still small, both $L_2$ and $L_\infty$ norms of the difference will be large. Since shifting of convergence zones is quite common when a Sound Speed Profile is altered, it is seen that point criteria[9] (such as $L_p$ norms) are not adequate for our needs.

## III. Quantitative Characterization of Curves

A typical transmission loss curve (Fig. 2) may be described (qualitatively or quantitatively) in terms of its typical characteristics:

i) Monotonic Element: If one were to "smooth out" all the convergence zones, so that the loss was principally spreading and attenuation, then what loss curve does one obtain?

ii) Existence of Convergence Zones: Most long-range propagation loss functions show zones, but there are exceptions. If there are convergence zones, then one may consider the next two characteristics.

iii) Convergence Zone Placement: This concerns the distance from the source to the first convergence zone, and the distances between the successive convergence zones. The distance between successive zones need not be constant, but in most cases, it will not vary radically.

iv) Convergence Zone Shape: This characteristic includes properites such as the geometric shape of the zone (on both sides of the caustic), the spread of the successive convergence zone widths, and the decay (or growth) of the successive convergence zones. Properties of the zones

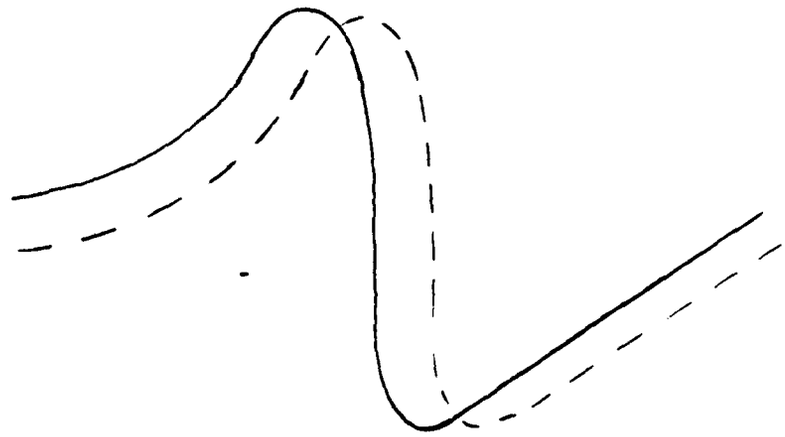

Figure 1. Shifted Caustic

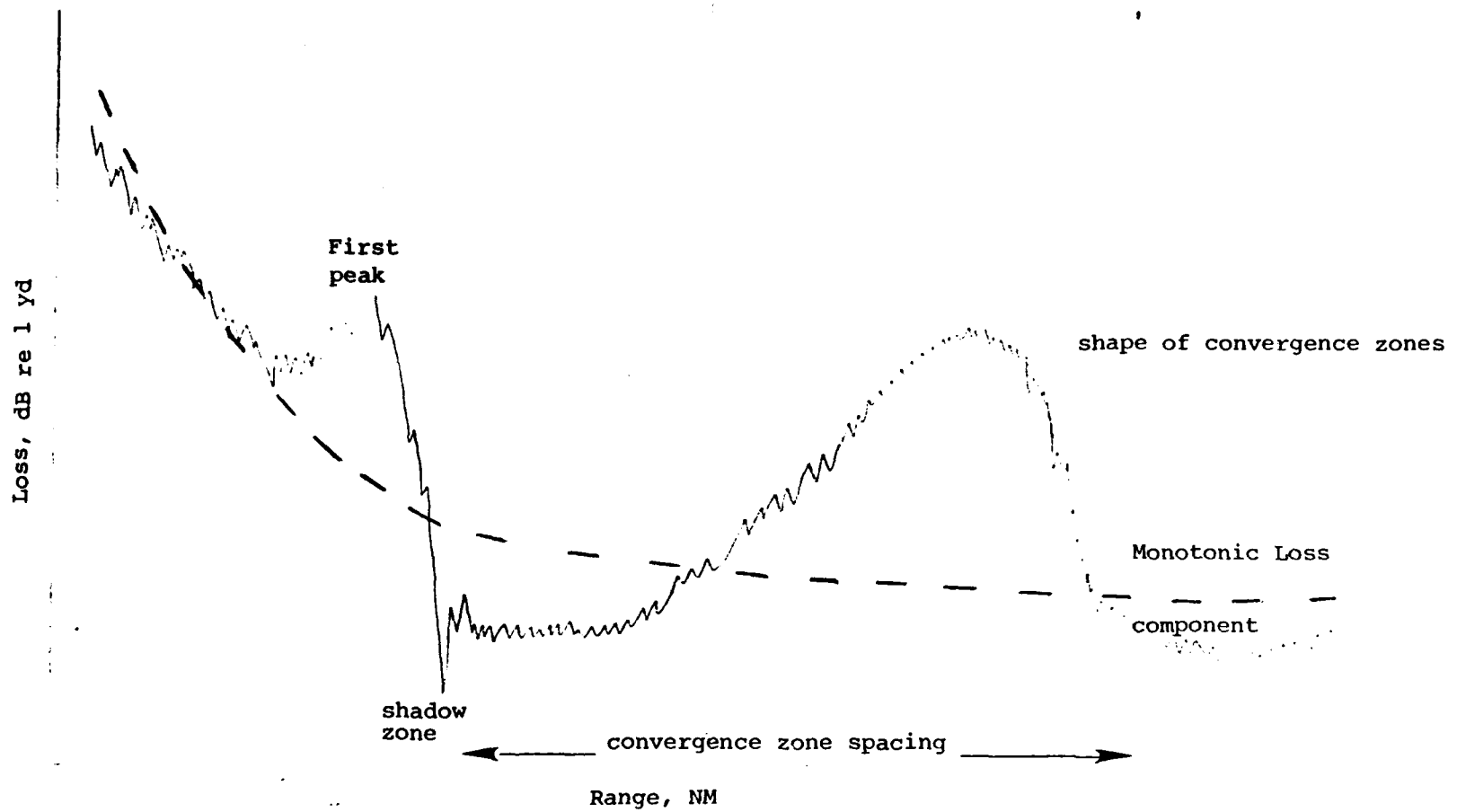


Figure 2. Typical TL curve showing descriptive elements

such as the difference in intensity between a convergence zone and the adjoining shadow zone might also be considered as characteristics of shape, but they will be dealt with when considering deviations from the monotonic component.

Each of these may be quantitatively described by a variety of methods, depending upon the amount of detail with which one wishes to work. An inadequate level of detail results in phenomena being lost through simplification, while an excessive level of detail results in phenomena being buried in myriads of numbers. Neither extreme is acceptable. The approach given below is based on analytic considerations in these four categories of characteristics.

## IV. Definitions

In this section, formal definitions are given for a number of variables and functions which will be used throughout the paper. For quick reference, a list of notation is also provided following the appendices.

Let $T_k(r)$, $k = 1, 2$ be transmission loss curves, which are given out to range $r_k$. One could consider that the domain of $T_k$ was the half-open interval $(0, r_k]$, but transmission loss data is not collected down to zero range, nor are long-range models always accurate at absurdly short ranges. Thus, we choose a $\delta>0$ and consider the transmission loss functions to begin at range $\delta$. Let $r_{12}$ be the minimum of $r_1$ and $r_2$ and we will always assume

$$\delta < r_{12} \quad .$$

Thus, the domain of $T_k$ will be the closed interval $[\delta, r_k]$. Let $\ell_k(r)$ be a monotonic loss function corresponding to $T_k(r)$, so that its domain is also $[\delta, r_k]$. Let $\ell_{12}(r)$ be a monotonic loss function corresponding to $T_1$ and $T_2$, where domain will be $[\delta, r_{12}]$.

(The derivation of $\ell_1$, $\ell_2$, and $\ell_{12}$ is found in the next section.) And, let $P_k(r)$, $P_{kk}(r)$ be the perturbation components, defined by

$$P_k(r) = T_k(r) - \ell_k(r)$$

$$P_{kk}(r) = T_k(r) - \ell_{12}(r)$$

As discussed in Chapter X, the perturbation component $P_{kk}(r)$ will not normally be used; we include it here for convenience of definition. It should also be noted that when functions of range (r) are explicitly stated, it is assumed that r is in nautical miles.

Now, we turn to the development of a weighting function for integration. Let f(r) be a weighting function defined on (0, $\infty$) which will be used to ensure that the analysis is not strongly dependent upon $r_k$. Ideally, f should be more-or-less level across the range of direct propagation, first convergence zones, first shadow zone, and second convergence zone. It should then drop off and approach zero asymptotically. Three typical forms for f are shown in Fig. 3.

The linear form

$$f(r) = \begin{cases} 1 & \text{for } r \le 70 \\ \frac{110-r}{40} & \text{for } 70 < r < 100 \\ 1/4 & \text{for } 100 \le r \end{cases}$$

is very convenient for computer calculation, but is a somewhat crude approximation, particularly in regard to the asymptote. The rational form

$$f(r) = 1/(1+x^4)$$

where

$$x = (r-30)/48$$

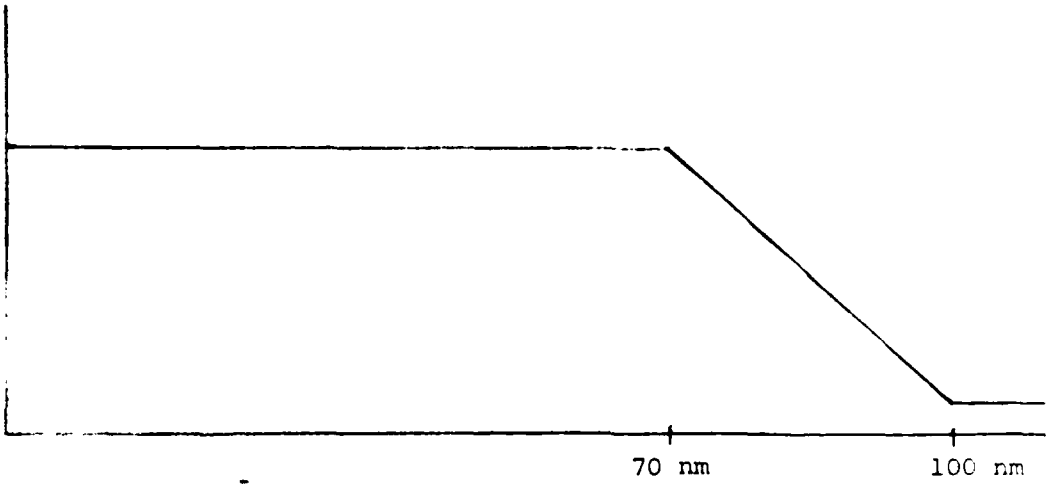


a) Linear approximation

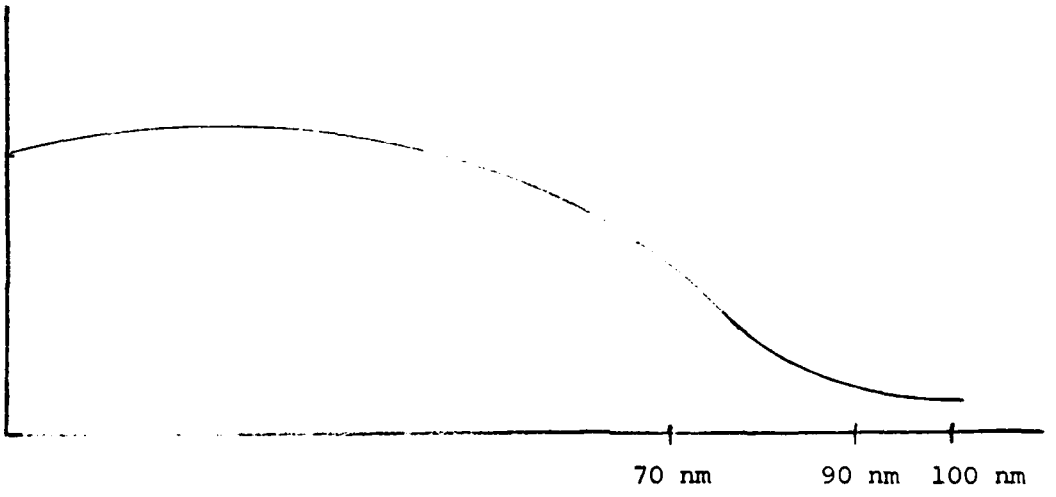


b) Rational Approximation

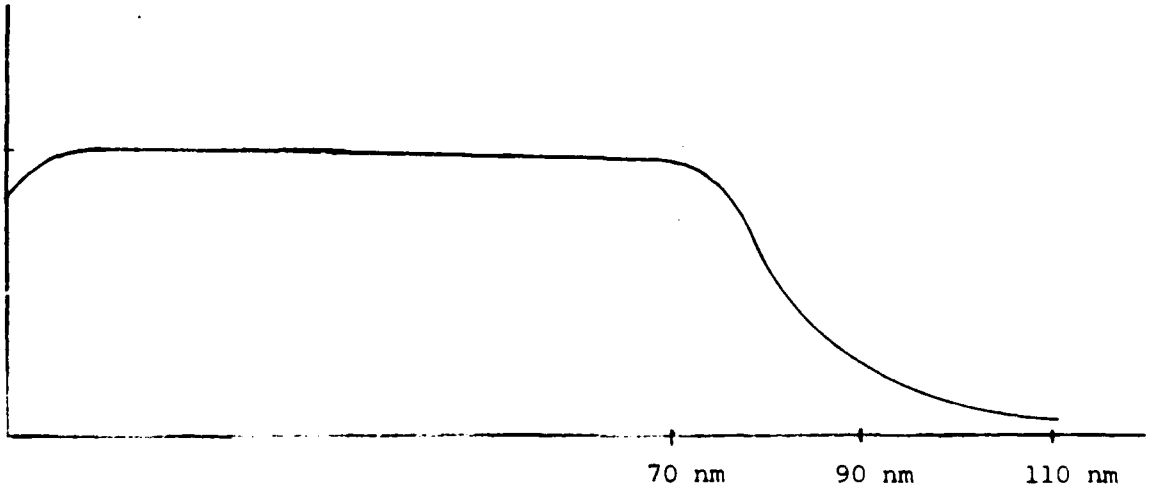


c) Ideal form

Figure 3. Three forms for the weighting function.

is vastly superior in this regard. A more precise representation of the weighting function (Fig. 3c) may be obtained using hyperbolic trigonometric functions, but the complexity of the computer calculations exceeds the marginal benefit gained over the rational approximation.

It was stated above that the shape of f was chosen so that the analysis would not be strongly dependent upon the values of the two $r_k$. This statement will now be explained. The analysis used in this paper is based on various integrals of the transmission loss functions. These integrals are usually algebraic combinations of the functions, hence, it suffices to consider the most elementary, i.e., a simple average.

$$\mu(r_1) = \frac{\int_{\delta}^{r_1} T_1(r)\,dr}{r-\delta}$$

It is apparent from Fig. 4 that this average is highly dependent upon the argument, for $\mu(\nu_1)$ differs considerably from $\mu(\nu_2)$. But, the analysis of propagation loss curves should not be unduely influenced by the amount of the curve (i.e., the range) which is known.[10] Therefore, integrals such as the simple average given above are not a good foundation upon which to build the theory. To avoid such a situation, a weighting function is introduced which goes to zero asymptotically as the range increases. Since we are dealing with long-range propagation modeling,[11] one may expect that most propagation loss curves will be known to ranges over 70 nm, and that a range of 110 nm is often attained. Thus, in this region, the weighting function should decrease substantially. One usually encounters the first and second convergence zones and the first shadow zone within 70 nm or so of the source, so that these primary characteristics will be weighted heavily. Conversely, many model runs are made to several hundred miles. But, if one is comparing two propagation curves, it is not clear that one could justifiably compare the finer properties of the curves at ranges of several hundred miles. Thus, the low weight given to these ranges is acceptable.[12]

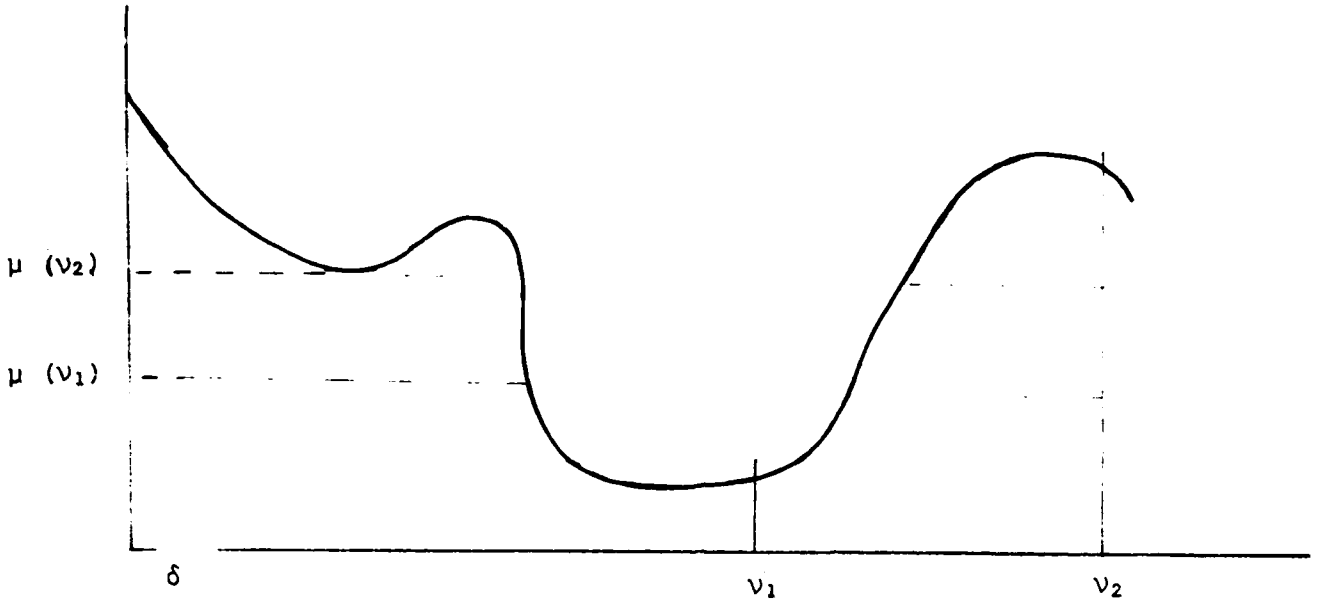


Figure 4. Dependence of μ upon $\nu_1$

V. The Monotonic Component

In this section, we investigate the spreading and attenuation properties of the loss curve. Let us assume that these two phenomena may be described by a function of the form

$$\ell_k(r) = b_k + \hat{b}_k \log r + \alpha r$$

where $b_k$ $\hat{b}_k$ are constants to be determined and $\alpha$ is the attenuation coefficient.[13] For any function $\ell$ of suitable domain, define the functional

$$\Theta_k(\ell) = \frac{\int_\delta^{r_k} (T_k(r)-\ell(r))^2 f(r)dr}{\int_\delta^{r_k} f(r)dr}$$

Then, we choose $b_k$, $\hat{b}_k$ (k=1, 2) such that $\ell_1$ minimizes $\Theta_1$ and $\ell_2$ minimizes $\Theta_2$. The function $\ell_k$ represents the best weighted least squares fit from this class of monotonic functions to the curve $T_k$. The function $\ell_k$ will be used as the descriptor of the monotonic component of $T_k$. In Chapter X, which deals with the comparison of two propagation loss curves, it will be necessary to use another curve which represents the spreading and attenuation of both loss curves. This common monotonic component will be a function $\ell_{12}$ of the above class,[14] and it will be the unique function which minimizes the functional

$$\Theta_{12}(\ell) \stackrel{d}{=} \Theta_1(\ell) + \Theta_2(\ell)$$

The three values

$$\Theta_1(\ell_1),\ \Theta_2(\ell_2),\ \Theta_{12}(\ell_{12})$$

are statistics which should be computed when comparing two curves. An efficient method for obtaining these quantities is given in

Appendix A. These are measures of the deviation of the curves from a monotonic loss function.

Another quantity of interest, to measure sudden rise or drop in the transmission loss curve, will be defined. If one wished to measure such a characteristic, then the difference would be

$$|T_k(r) - T_k(r+\sigma)|$$

where $\sigma$ was some small amount (e.g., several miles). Thus, one might consider a measure such as

$$\max\{|T_k(r)-T_k(r+\sigma)|: \delta \le r \le r_k - \sigma,\ 0 \le \sigma \le \tilde{p}\}$$

where $\tilde{p}$ is a constant (e.g., 10 nm). Unfortunately, while this is a very good measure, it has the one drawback of being, in certain cases, strongly dependent upon $r_k$. Thus, one chooses a less meaningful but more stable measure

$$\chi_k = \max\{|T_k(r)-T_k(r+\sigma)-\hat{b}_k \log(1+\frac{\sigma}{r})-\alpha\sigma|\sqrt{f(r)f(r+\sigma)}:$$

$$\delta \le r \le r_k - \sigma,\ 0 \le \sigma \le \tilde{p}\}$$

Let $\sigma_k$ be the value of $\sigma$ which maximizes the functional.

## VI. Convergence Zones: To be or not to be

The decision as to whether or not a transmission loss curve has convergence zones would appear to be relatively straightforward: an acoustician can make such a determination by visual inspection (cf. Fig. 5). But, such a determination may be difficult when one has points arising from either measured data or a coherent model which exhibit a significant scatter, so that the presence or absence of slight convergence zones is hidden by the "noise" (Fig. 6).[15]

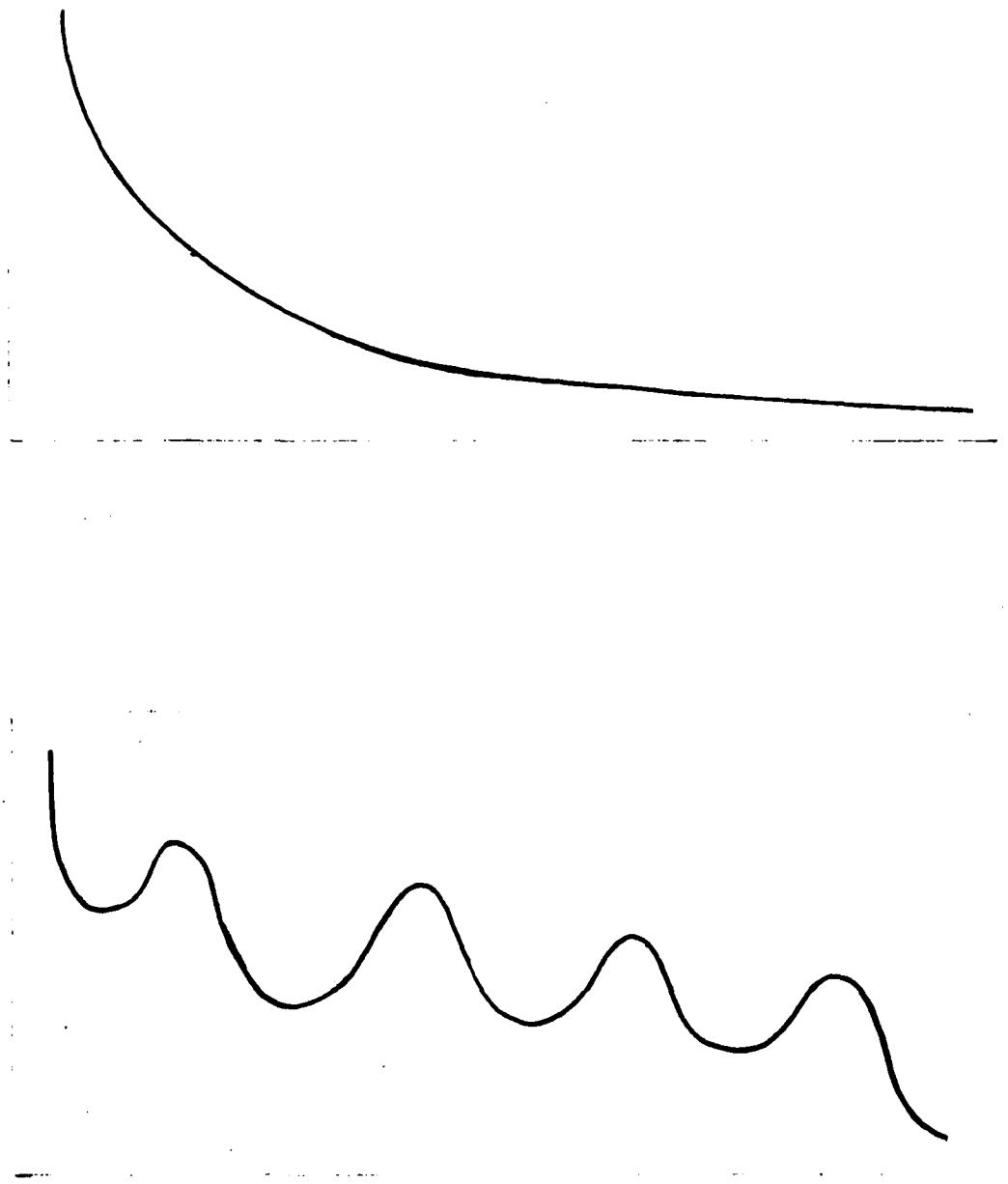

Figure 5. Obvious presence and absense of convergence zeros

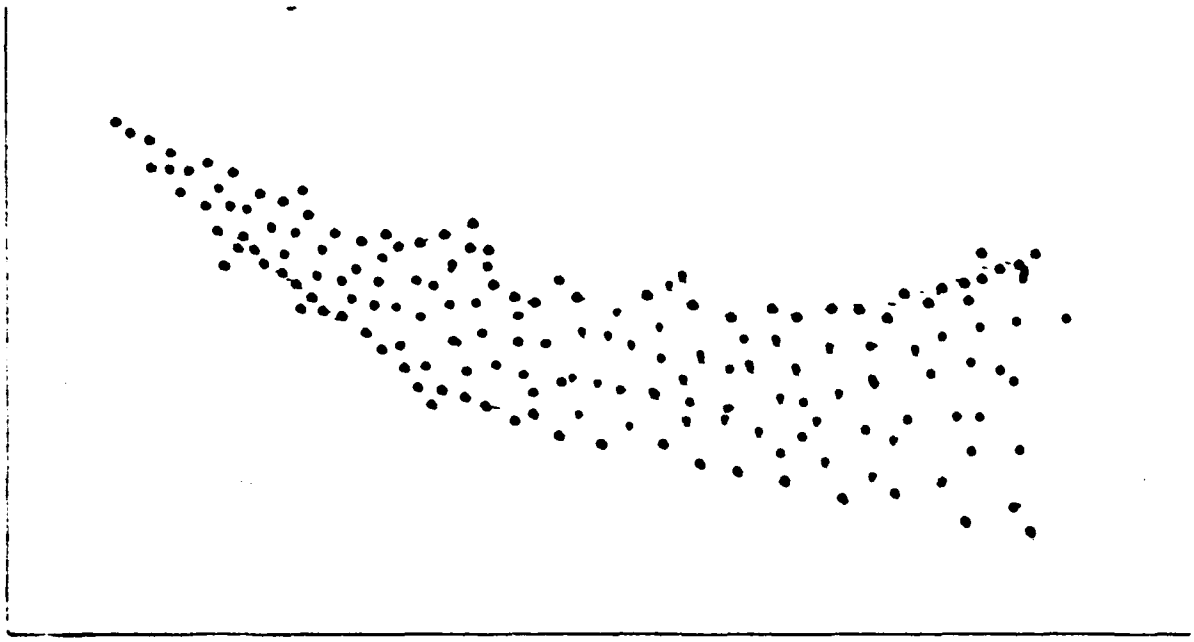

Figure 6. Discrete pts, TL vs range.

One needs a method of discrimination which the computer can perform, and a three-step procedure is used. To determine if $T_1(r)$ has convergence zones, the first step is to examine $\Theta_1(\ell_1)$, which is a measure of the deviation of $T_1(r)$ from $\ell_1(r)$. Such deviation may be due to either data scatter (cf. Fig. 6) or to convergence zones. Let $\tilde{\kappa}$ be a threshold such that if

$$\Theta_1(\ell_1) < \tilde{\kappa}^2$$

then one immediately concludes that convergence zones are not present. Let $\kappa$ be a threshold such that if

$$\tilde{\kappa}^2 \leq \Theta_1(\ell_1) < \kappa^2$$

then it is very probable that convergence zones are not present, but the second step should be used for this determination. Reasonable values for $\tilde{\kappa}$ and $\kappa$ might be 2 dB and 2.5 dB, respectively.

The second step is examination of $\chi_\kappa$ to try and determine whether a small amount of deviation is due to data scatter or convergence zones. This is only done when $\Theta_1(\ell_1)$ lies between the two thresholds. If

$$\Theta_1(\ell_1) \geq \kappa^2$$

then this step should be ignored and step three used for determination. If $T_1(r)$ was identical to its monotonic component, then $\chi_1$ would be zero. Thus, one may choose a threshold $\tilde{\theta}$ and state that if

$$\chi^2_1 < \tilde{\theta}^2 \Theta_1(\ell_1)$$

then the variation of $T_1$ from $\ell_1$ is a slowly-varying function; too slowly varying to be convergenze zones.[16] This threshold is very difficult to estimate; a starting value might be 1/3. And, a threshold $\tilde{\sigma}<\tilde{p}$ is used to test for short-range fluctuations. If

$$\sigma_1 < \tilde{\sigma}$$

then is assumed that we are dealing with short-range fluctuations rather than convergence zones. Ideally, we should have

$$\tilde{\sigma} << \tilde{p} .$$

But, the transmission loss curve $T_1$ is entered at discrete points, and from the definition of $\chi_i$, it is obvious that $\sigma_i$ will be either $\tilde{p}$ or the distance between two of these discrete points. For short-range fluctuations, $\sigma_1$ will not be $\tilde{p}$ (cf. Fig. 21a), so $\sigma_1$ will be a distance between some pair of input points. Thus, the test with $\tilde{\sigma}$ is nontrivial only if $\tilde{\sigma}$ is greater than the distance between adjacent points of the tabulated transmission loss data. If transmission loss data was given every 10 km(=6.2 nm) and $\tilde{p}$ is 10 miles, then it is obvious that we cannot have both

$$6.2 \leq \tilde{\sigma} < 10$$

and

$$\tilde{\sigma} << 10 .$$

Therefore, this criteria may be difficult to successfully implement if the grid spacing of the tabulated transmission loss is large. If $\sigma_1$ is greater than that threshold, then one would proceed to step three.

The third step is to determine whether the suspected convergence zones really are significant zones. This step, which is the final one of the convergence zone determination, is done in a constructive manner; i.e., we find the first convergent zone. If the algorithm to find the first zone fails, one assumes that no convergence zones exist. This algorithm is described in the next section, Convergent Zone Placement. If no such zone is detected, then the characterization of the propagation loss curve is limited to its

monotonic component, the mean square deviation from that component, and the maximum variation over an interval.[17]

## VII. Convergence Zone Placement

In this section, we restrict attention to the problem of determining the location of each convergence zone (the peak, not the full zone). From this, we will develop measures which can be used to characterize convergence zone placement.

An obvious way to obtain the distance to the initial zone, and the spacing of successive convergence zones, is to take the (local) maxima (Fig. 7). In actual use, this may be done easily by eyeball, but not by the computer, for many transmission loss curves[18] are very jagged (Fig. 8).

Merely identifying the maximum value within a range of one convergence zone is possible, but this will lead to erroneous identification in certain instances (e.g., Fig 9). A straightforward solution to this is to use a running weighted average of the transmission loss curve, not the curve itself. Then, the local maxima of the weighted sliding average will correspond to the convergence zone peaks.[19] To obtain such a running average, choose a function $\omega_R(r)$ such as that in Fig. 10 as the weighting kernel. Appendix I discusses typical forms for $\omega_R(r)$. Using this function, define

$$\Phi_k(R) = \int_{\delta}^{r_k} P_k(r)\omega_R(r)f(r)dr$$

as the averaged curve.

Since the problem is to identify the first peak, a range $R_o$ which is past the (expected) position of the peak is chosen, and $\Phi_k(R)$ is examined on the interval $[\delta, R_o]$. This function should look more-or-less like that of Fig. 11. The desired solution is a local maxima,[20] i.e., a point where $\Phi'_k(R)$ changes sign and $\Phi''_k(R)$ is negative. This value of R will be the location of the initial peak; call it $R_1$. When it is important to designate it as the initial peak of $T_k(r)$, it will be denoted $R_{1,k}$. One could continue

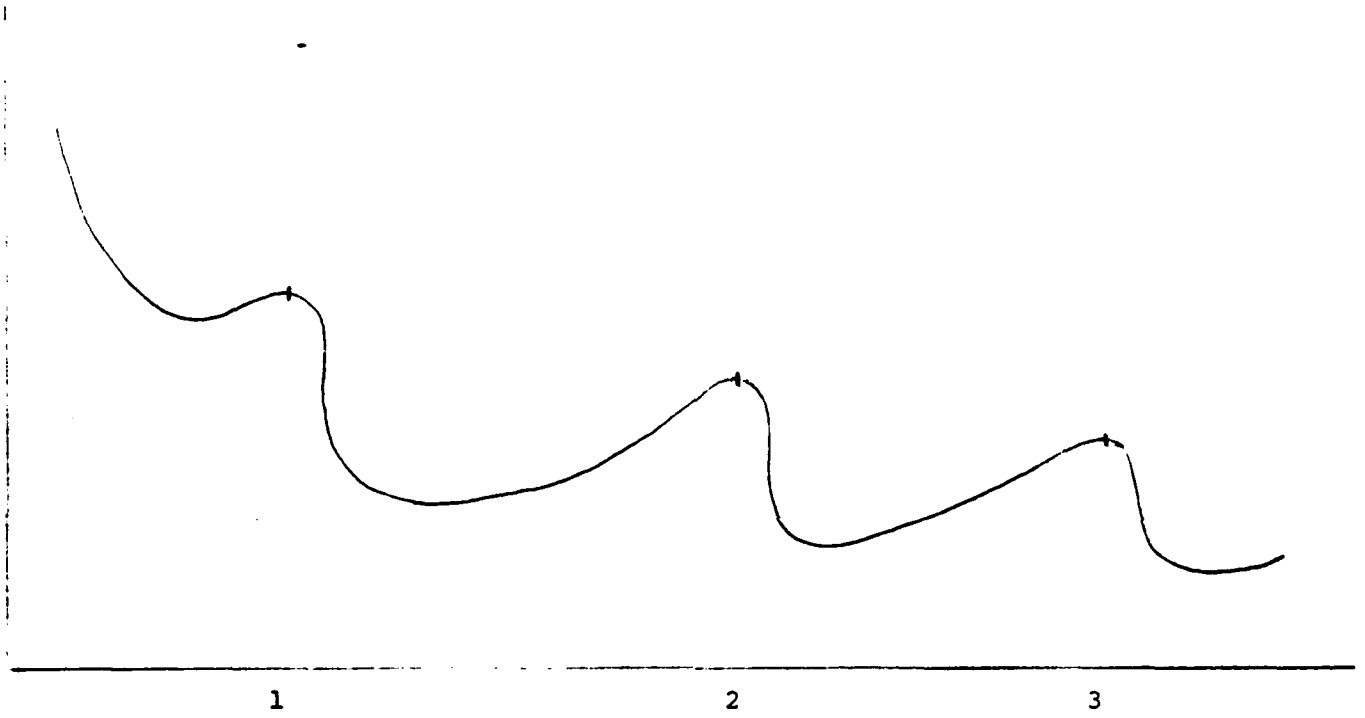


Figure 7. Mark-I eyeball method of determining cz peaks.

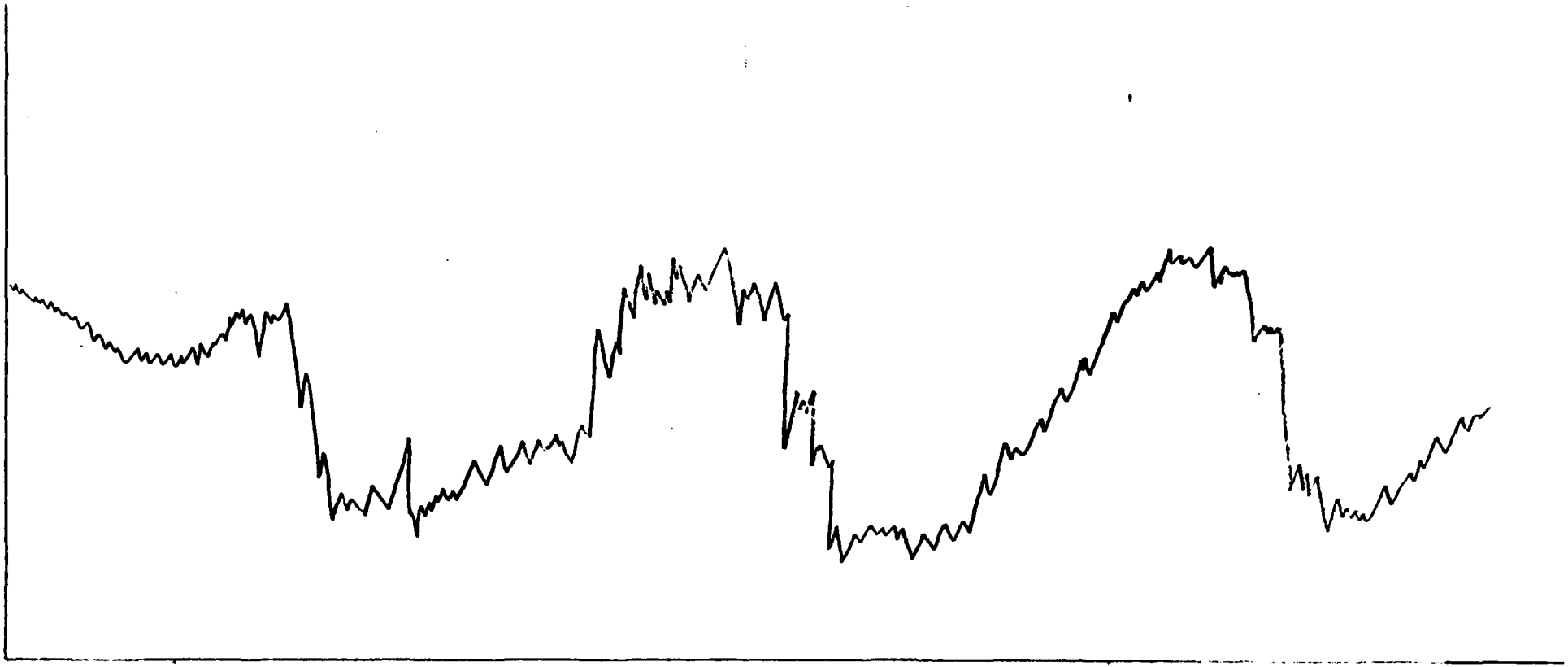

Figure 8. Realistic TL curve

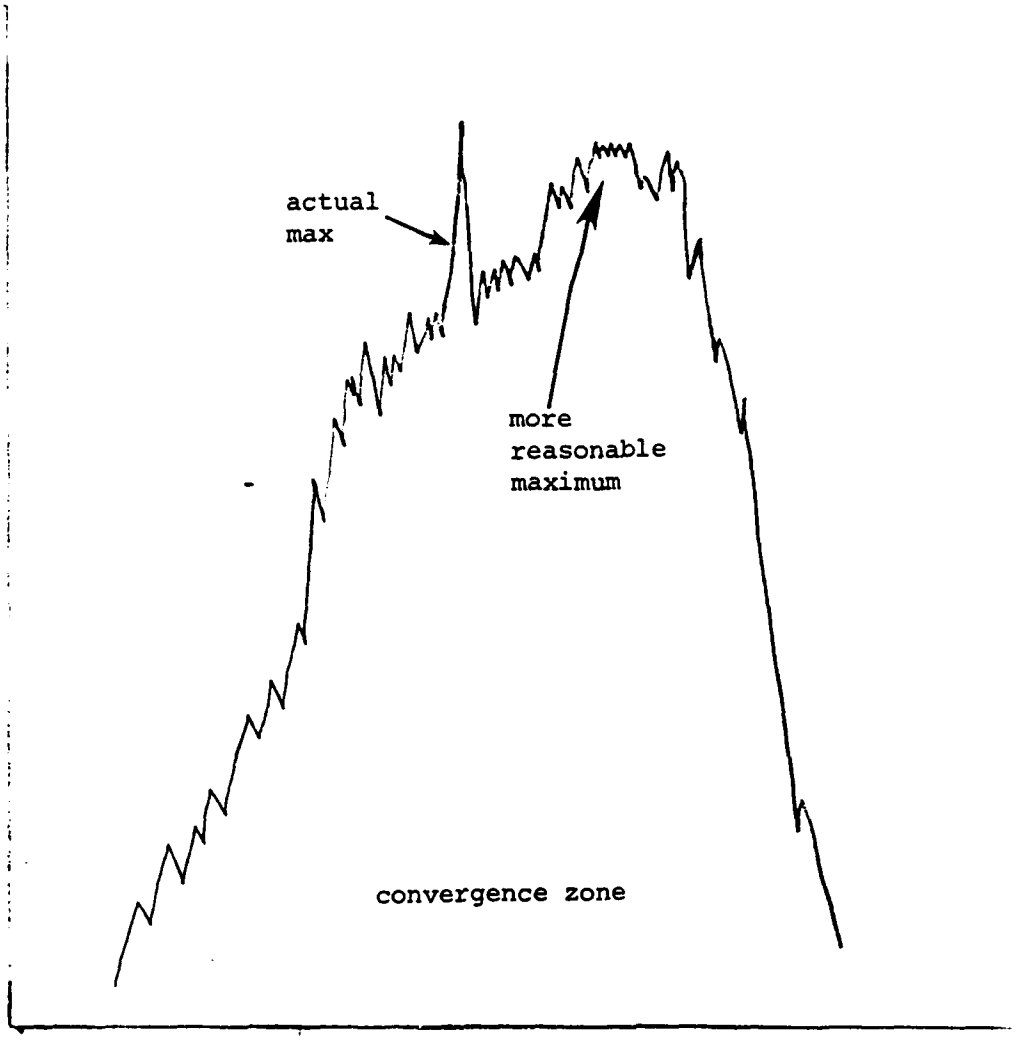


Figure 9. Situation in which actual maximum of TL curve is not best estimate of convergence zone.

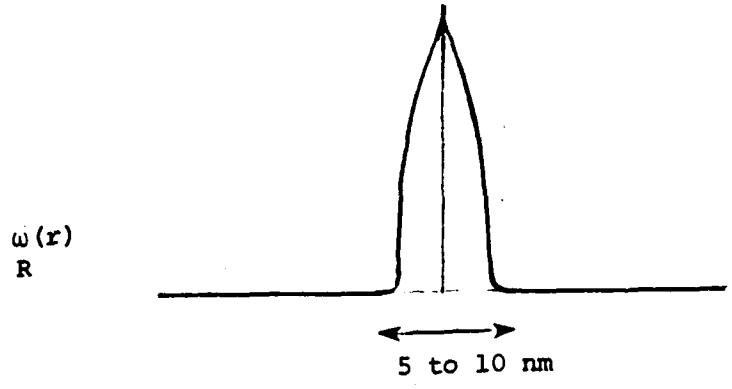


Figure 10. Weighting function

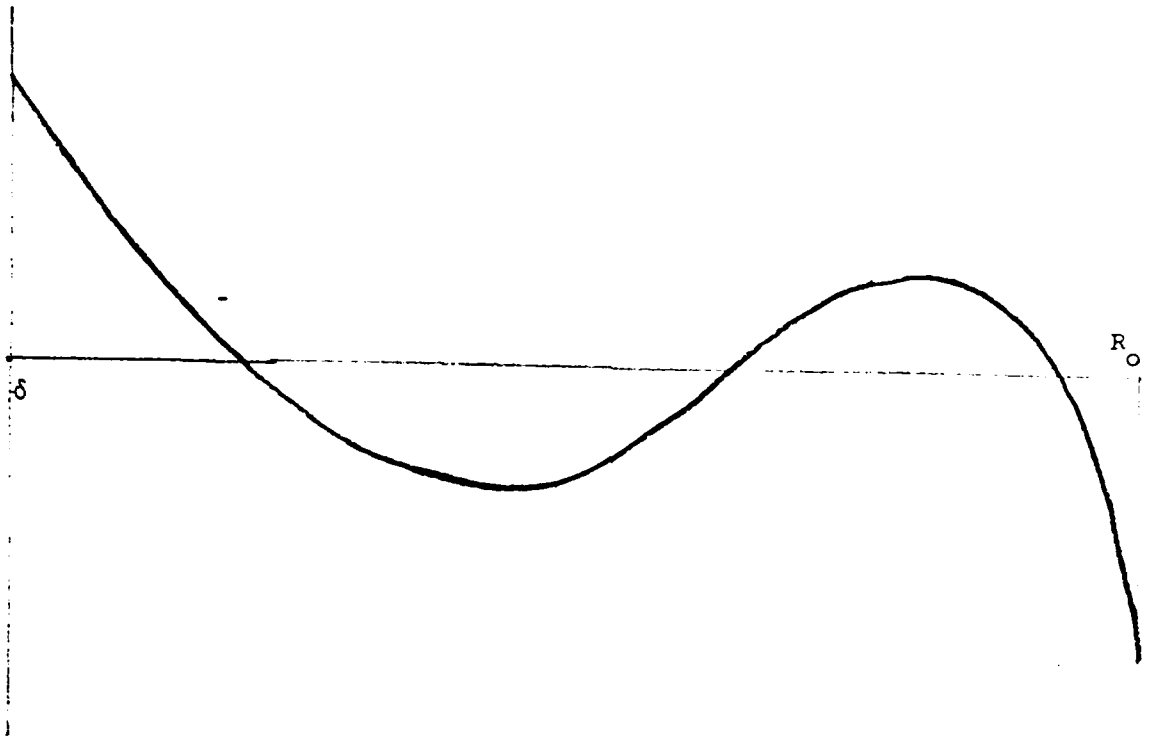


Figure 11. $\Phi_k(R)$ for first zone.

this method to locate the successive peaks $R_2$, $R_3$, etc., but such a method is fraught with numeric instabilities which may easily result in false "convergence zones."

It should be pointed out that one may have a peak where the transmission loss is still monotonic,[21] as in Fig. 12.

From Appendix B it is seen that the spacing between convergence zones is not (in general) constant, but the deviation from a constant is rather small. Therefore, rather than compute the intervals between the successive convergence zones, the average interval between convergence zones will be estimated and that will be the descriptor.

If one writes

$$\Delta_j R = \Lambda + \tilde{\varepsilon}_j$$

where the $\tilde{\varepsilon}_j$ are small and "average out" to zero, then $\Lambda$ will the the desired spacing estimate. To this end, define the function[22]

$$Q_\lambda(r) = \sum_{j=0}^{\infty} \omega_{R_1+j\lambda}(r)$$

for $\lambda>0$. Then, the value $\lambda_k$ which is a local maximum for the functional

$$\Omega(\lambda_k) = \int_\delta^{r_k} P_k(r) Q_{\lambda_k}(r) f(r) dr \Big/ \int_\delta^{r_k} Q_{\lambda_k}(r) f(r) dr$$

will be the estimate of $\Lambda$ for the transmission loss curve $T_k(r)$.[23] Since

$$\delta \le R_1 \le R_0 \le r_k$$

the denominator of this function cannot be zero.[24,25] Define

$$\Omega_{k,\infty} = \int_\delta^{r_k} P_k(r) \omega_{R_1}(r) f(r) dr \Big/ \int_\delta^{r_k} \omega_{R_1}(r) f(r) dr$$

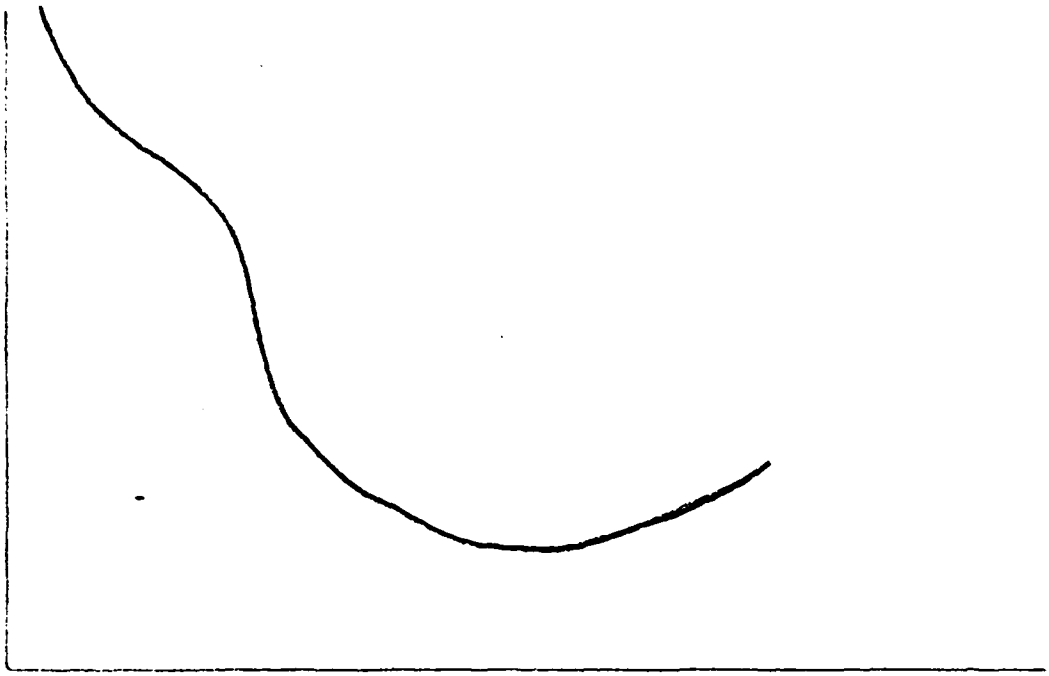

Figure 12. Case in which first 'peak' is not a local maximum.

then

$$\Omega(\lambda_k) = \Omega_{k,\infty}$$

if

$$\lambda_k > r_k + \varepsilon - R_1$$

Also,

$$\lim_{\lambda_k \downarrow 0} \Omega(\lambda_k)$$

exists[26] and except for some pathological cases, it is less than $\Omega_{k,\infty}$. So, a true maximum will generally exist,[27] and Fig. 13 illustrates a common case for which this is true.[28] But, Fig 13 also illustrates a case where the true maximum is not the desired maximum.[29] Figure 14 shows another case where the true maximum is not the desired maximum.[30]

It is clear from these examples that when $\lambda_k$ is chosen, it should not be a global maximum, but rather a local maximum. Thus, an interval must be chosen so as to span only one convergence zone at a time,[31] and the function is examined on such an interval.

In summary, this chapter has given the techniques to determine the descriptors $R_{1,k}$ and $\lambda_k$ of the convergence zone placement of $T_k(r)$.

## VIII. Convergence Zone Shape

In this section, a quantitative measure is associated with the shape of a convergence zone.[32] There are a number of measures one could devise; those chosen are easily implementable. It is anticipated that the other measures (e.g., monotonic component, deviation from monotonic component, convergence zone spacing) will prove more significant in practice.

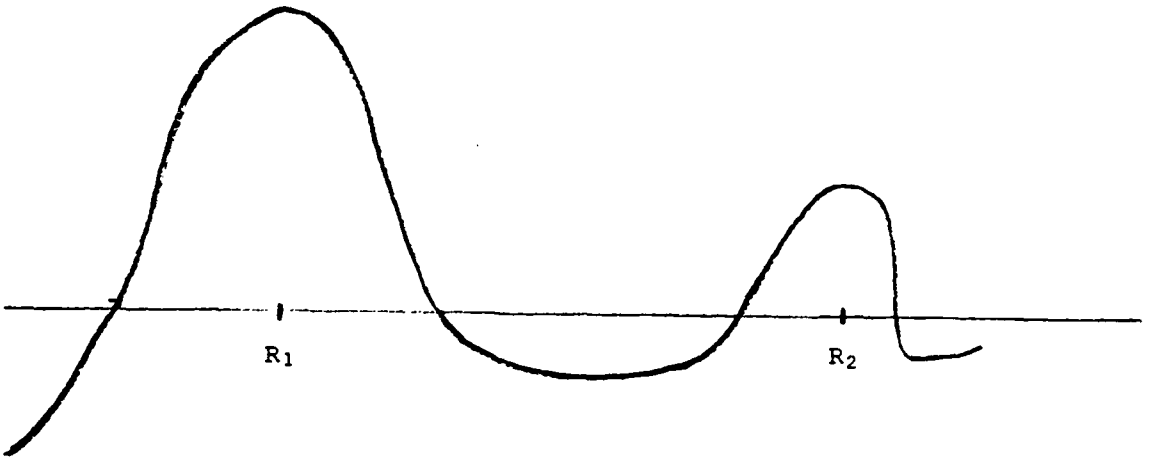


Figure 13. Maximum peak of $P_k$ is at $R_1$

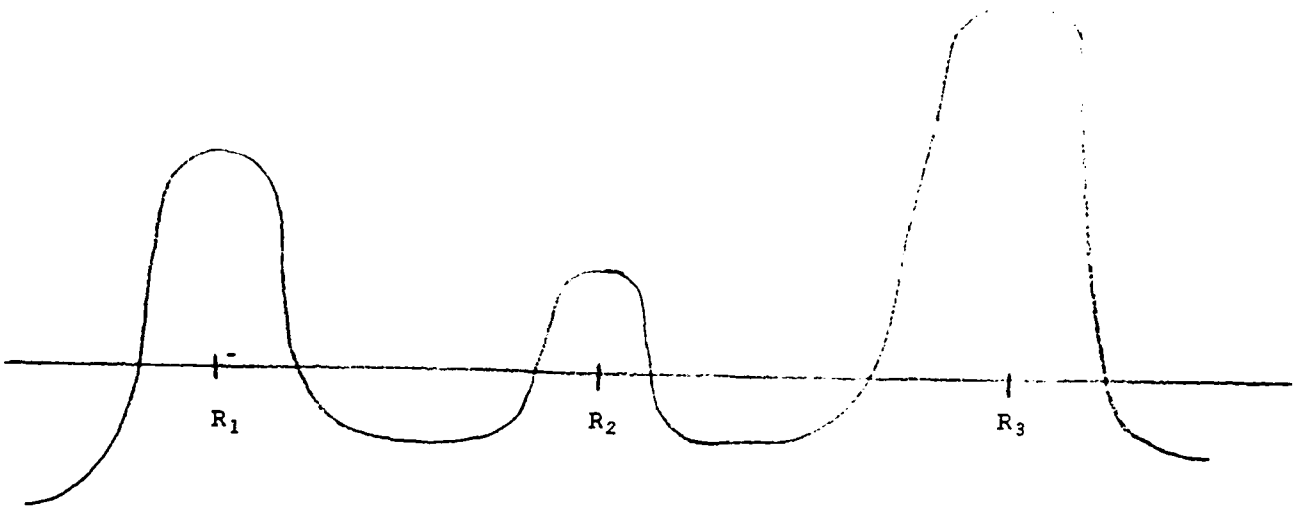


Figure 14. A case where the second peak of the perturbation $P_k$ is much smaller than the third.

One could attempt to describe the shape of each convergence zone, or describe the overall, or "average" shape of the convergence zones. Or, one may merely describe the shape of a selected set of zones (e.g., the first two). It is this last approach that will be taken, although the technique used is basic to all three approaches.

Let $R_j$ be the (averaged) distance to the j-th convergence zone from the source, i.e.,

$$R_j = R_1 + (j-1)\lambda_k$$

and consider the shape of the j-th peak. The shape will be modeled by the function

$$\Psi_k(r) = \begin{cases} d_1 + d_2 x + \dfrac{d_3}{x+d_o} & r \geq R_j \\ d_4 + d_5 x + \dfrac{d_6}{x-d_o} & r < R_j \end{cases}$$

where $d_i$ are constants and

$$x = r - R_j \ .$$

The determination of these coefficients is found in Appendix Δ. Although there appear to be seven coefficients, one of them is chosen beforehand, and the condition $\Psi_k \varepsilon C^1$ is imposed so that in reality there are only four "degrees of freedom." The four (independent) coefficients may be used as shape descriptors, or all seven may be used. If $d_5 \leq 0$ or $d_2 \geq 0$, however, the shape of the convergence zone is not suitable for description by the form $\Psi_k$; hence, the coefficients calculated should not be used.

Therefore, one obtains either a set of shape coefficients, or an indicator that the shape is significantly different from the anticipated form.

This completes the quantitative measures of a single transmission loss curve. The next two chapters will deal with comparisons of two such curves.

## IX. Comparison of Measures of Transmission Loss Curves

If one is given two (or more) transmission loss curves, a natural way to compare them would be to compare the various measures of those curves which were developed above.

The measures defined previously may be listed for convenience

$$\ell_k$$

$$\Theta_k(\ell_k)$$

$$\chi_k$$

$$R_{1,k}$$

$$\lambda_k$$

$$\Omega_{k,\infty}$$

$$\Psi_k$$

To compare the monotonic components $\ell_1$ and $\ell_2$, one might wish to just compare their coefficients, but such a procedure can be misleading, for the two curves may be quite close over the common interval $[\delta, r_{12}]$, but have rather different coefficients.[33] A better comparison is obtained by computing

$$T_\alpha = \frac{\int_\delta^{r_{12}} (\ell_1(r)-\ell_2(r))^2 f(r)dr}{\int_\delta^{r_{12}} f(r)dr}$$

This integral is most efficiently computed by numeric quadrature rather than by analytic evaluation.

This seems to be a rather simple formulation, and taking the d
criminant, gives

$$\beta_7^2 - 4\beta_6\beta_8 = \{2\gamma\upsilon\sin\xi\}^2\beta_9^2$$

where

$$\beta_9^2 = \{1-\gamma^2\upsilon^2+\tfrac{1}{4}\gamma^2\upsilon^2\xi^2\}\sin^2\xi - \xi(1-\gamma^2\upsilon^2)\cos\xi\sin\xi$$

The roots of the quadratic are

$$\psi = \frac{-\beta_7 \pm 2\gamma\upsilon\beta_9\sin\xi}{2\beta_8}$$

Thus, to compute the caustics, one uses the parameter $\xi$, comp
$\psi$, then $\Xi$, then x and y, remembering that most of the functio
multivalued,[44] i.e.,

$$\Xi = \sqrt{1-\gamma^2\upsilon^2-\xi\psi}$$

$$x = \gamma^{-1}\xi\sqrt{\xi\psi}$$

$$y = \gamma^{-1}\{\Xi\sin\xi-\gamma\upsilon\cos\xi\}$$

Now, for $\xi$ a positive integral multiple of $\pi$, there is a (rea
cusp on the caustic, which may be obtained by power series de
ment. Let

$$\xi = m\pi - \eta^2 \qquad m\epsilon Z^+$$

then

$$\beta_6 = \beta_2^2-\beta_2\eta^4 + \tfrac{1}{3}\eta^8 - \tfrac{2}{45}\eta^{12} + O(\eta^{16})$$

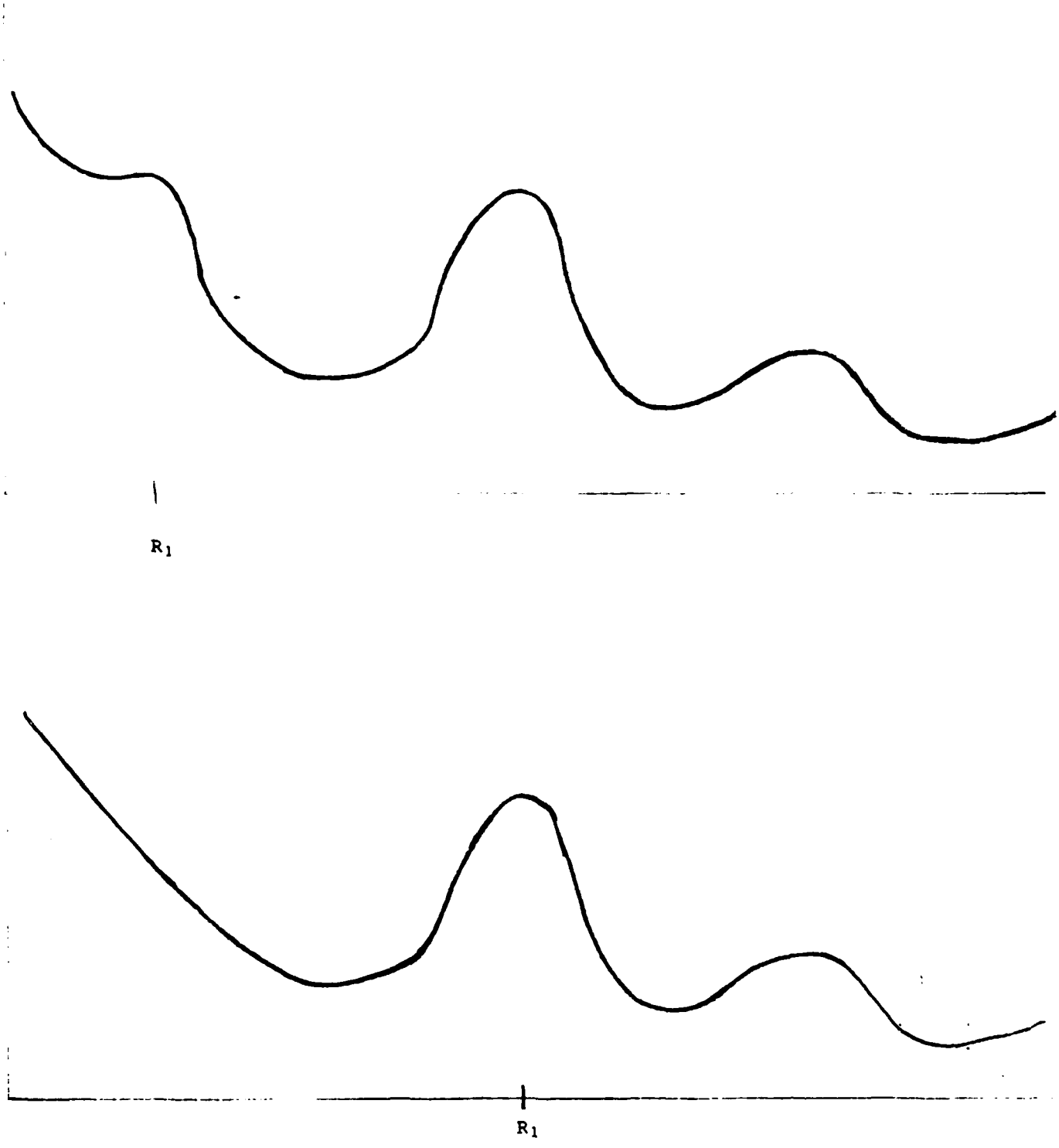


Figure 15. Two transmission loss curves which are similar but with vastly different $R_1$'s.

$$T_\delta = \min\{|R_{i1}-R_{j2}|: i,j=1,2\}$$

and let $i_o$, $j_o$ be the indices which give this minimum. It will also be useful to form the difference of the zone spacings

$$T_\varepsilon = \lambda_1 - \lambda_2 .$$

These two measures indicate (by their proximity to zero) how the convergence zone spacing of the two curves compare.

In regard to the limiting values of the $\Omega_k(\lambda)$'s, one might be tempted to follow the previous procedures and just take the difference

$$\Omega_{1,\infty} - \Omega_{2,\infty}$$

But, since these represent the level of the first peak above the monotonic component, the value of this measure is not immediately obvious. First, it should be remarked that if

$$i_o \neq j_o$$

then no tests should be performed on $\Omega_{k,\infty}$ since they correspond to different peaks of the two curves. If the indices are equal, then form the ratio

$$T_\zeta = \frac{\Omega_{1,\infty}}{\Omega_{2,\infty}}\sqrt{\frac{\Theta_2(\ell_2)}{\Theta_1(\ell_1)}}$$

This is a measure of how well the first peaks correspond in light of the overall deviations. If $T_\zeta$ is close to 1, agreement is good.

Now, we consider the shapes of the zones. One could compare the curves zone by zone, but this is probably more complicated than the situation requires. It is better to confine attention to one or two convergence zones: the first peak, the second peak, or both.

The choice of whether to use the first or second peak is difficult since each has certain advantages, hence the use of both. As with the previous test, this one should only be done if $i_o = j_o$ in the $T_\delta$ calculation. One then uses a measure of the form of an integral of weighted squared difference in the shapes, adjusted for possible differing levels, viz.

$$\min_{\phi} \frac{\int_s^t \hat{\omega}_o(x)\,(\Psi_1(x+R_{j1})-\Psi_2(x+R_{j2})+\phi)^2 dx}{\int_s^t \hat{\omega}_o(x)dx}$$

where

$$s = \max_k \ (\delta - R_{jk})$$

$$t = \min_k \ (r_k - R_{jk})$$

But, this is rather unwieldy, and if $\hat{\omega}$ has a reasonably small support (e.g., $\varepsilon<15$ nm., cf. App. Γ) and $r_{12}$ is not very small (e.g., $r_{12}>$ 60 nm), then for most transmission loss curves, the above functional is equal to

$$T_\eta(j) = \min_{\phi} \frac{\int_{-\infty}^{\infty} \hat{\omega}_o(x)\,(\Psi_1(x+R_{j1})-\Psi_2(x+R_{j2})+\phi)^2 dx}{\int_{-\infty}^{\infty} \hat{\omega}_o(x)dx}$$

For those transmission loss curves satisfying the above assumptions, but where the above functional is not equal to the first form, the forms are usually so close that the difference is negligible. The evaluation of this measure, in closed form, is given in Appendix E. The smaller this measure is, the closer the shapes of the convergence zones are.

This completes the measures based on the measures of the individual transmission loss curves.

X. Measures Based on Two Curves

In addition to the indicators based on comparison of measures of the individual curves, there are useful measures which can only be formed from considering several transmission loss curves at once. For the case of two loss curves,[36] some of these will be given.

The obvious measure, which has already been introduced, is the $L_p$ norm. Thus, we form a weighted norm

$$T_\theta(p) = \left\{ \frac{\int_\delta^{r_{12}} |T_1(r) - T_2(r)|^p f(r)\,dr}{\int_\delta^{r_{12}} f(r)\,dr} \right\}^{1/p}$$

and evaluate this for p=1 and p=1/2. The first (p=1) gives the (weighted) area between the curves, normalized by length of the common domain of the curves. The use of a value of p less than 1 results in a measure which is less sensitive to great divergences (such as caustics) and quite sensitive to the small devaitions between the curves. But, the integral (for p=1/2) cannot be easily given any physical meaning.

To investigate shift in convergence zones, one might be tempted to consider choosing $\tau$, where

$$0 \le \tau < r_{12} - \delta$$

in order to minimize

$$\frac{\int_\delta^\rho (P_1(r) - P_2(r+\tau))^2 (f(r) f(r+\tau))^{1/2} dr}{\int_\delta^\rho (f(r) f(r+\tau))^{1/2} dr}$$

or to maximize

$$\frac{\int_\delta^\rho P_1(r) P_2(r+\tau) (f(r) f(r+\tau))^{1/2} dr}{\int_\delta^\rho (f(r) f(r+\tau))^{1/2} dr}$$

where

$$\rho = r_{12} - \tau$$

But, unfortunately, the first form is not nearly as good a measure of shift as $T_\delta$ is, and the second form is even worse. The second form, which is based on a correlation concept, is highly unsatisfactory as a shift measure. But, the perturbation components $P_k(r)$ of the transmission loss curves are not periodic functions.[37] There are a number of phenomena that are not present with periodic functions which can affect this form, in some cases rather drastically. Neither of the two estimates for $\tau$ obtained from optimizing these two forms need be reasonable estimators of the shift. Thus, neither form will be used; we have discussed them merely due to their rather extensive use in other areas (e.g., signal processing).

If the measure $T_\varepsilon$ is not small (e.g., $T_\varepsilon > 8$ nm) then one may wish to examine the shape of the convergence zone--shadow zone cycles of the two curves, scaled so the convergence zones coalesce. Towards this end, let $V_k$ be the linear transformation taking the first peak $R_{1k}$ into 0 and the second peak $R_{2k}$ into 1, viz

$$V_k(R_{1k}) = 0$$

$$V_k(R_{2k}) = 1$$

or

$$V_k(r) = (r-R_{1k})/\lambda_k$$

These linear transformations take the range onto a new interval, on which the peaks of the $P_k$'s coalesce. The new curves are then given by

$$G_k(v) = P_k o V_k^{-1}(v)$$

and their common domain $[t_1, t_2]$ is given by the intersection

$$[t_1, t_2] = [V_1(\delta), V_1(r_1)] \cap [V_2(\delta), V_2(r_2)]$$

Note that since

$$t_1 \leq 0$$

$$t_2 \geq 1$$

this interval is not empty. Define the scaled weighting function

$$\zeta_k(v) = \sqrt{f_k \circ V_k^{-1}(v)}$$

then a useful measure of the similarity of shape is

$$T_1 = \min_{\phi} \frac{\int_{t_1}^{t_2} (G_1(v) - G_2(v) - \phi)^2 \zeta_1(v) \zeta_2(v) dv}{\int_{t_1}^{t_2} \zeta_1(v) \zeta_2(v) dv}$$

which may be reduced to a numeric quadrature by proceeding as was done in Appendix E, i.e., let

$$\hat{E}_q = \int_{t_1}^{t_2} (G_1(v) - G_2(v))^q \zeta_1(v) \zeta_2(v) dv$$

for q=0, 1, 2. Then

$$T_1 = \{\hat{E}_2 \hat{E}_0 - \hat{E}_1^2\} / \hat{E}_0^2$$

The smaller $T_1$ is, the closer the geometric shape of the convergence zones of the two curves will be. Of course, if any of the requisite parameters (e.g., $R_{1,k}$, $\lambda_k$) could not be calculated with confidence, then this measure cannot be evaluated.

Now one might wish to compute characteristics of a pair of transmission loss curves by first estimating $\ell_{12}$ and $\Theta_{12}(\ell_{12})$ of the curve, and then using $P_{kk}(r)$ rather than $P_k(r)$ in the calculation of the various quantities in Chapter VII and VIII. Such a technique has value when one of the transmission loss curves is defined over a rather short interval (in comparison to the other) and both curves are a'priori believed to be similar. But, this is a refinement whose complications are not worth considering at this point.

However, we do mention one measure based on $\ell_{12}$, viz

$$T_K(k) = \frac{\Theta_k(\ell_k)}{\Theta_{12}(\ell_{12})}$$

which is a measure of how well the individual monotonic components compare with the component $\ell_{12}$. The sum

$$T_K(3) = T_K(1) + T_K(2)$$

is often more handy to use in practice. Note that

$$0 \leq T_K(k) \leq 1$$

for

$$k = 1, 2, 3 .$$

The closer $T_K(3)$ is to 1, the better the $\ell_{12}$ component describes both curves, and the closer their individual monotonic components are. In a sense, $T_K(3)$ measures much the same characteristic as $T_\gamma$, but there are unusual situations in which one of these measures is numerically unstable (i.e., a different tabular representation of a wierd transmission loss curve could significantly alter the measure) while the other one will remain stable. Thus, it is preferable to compute both $T_\gamma$ and the $T_K(k)$'s.

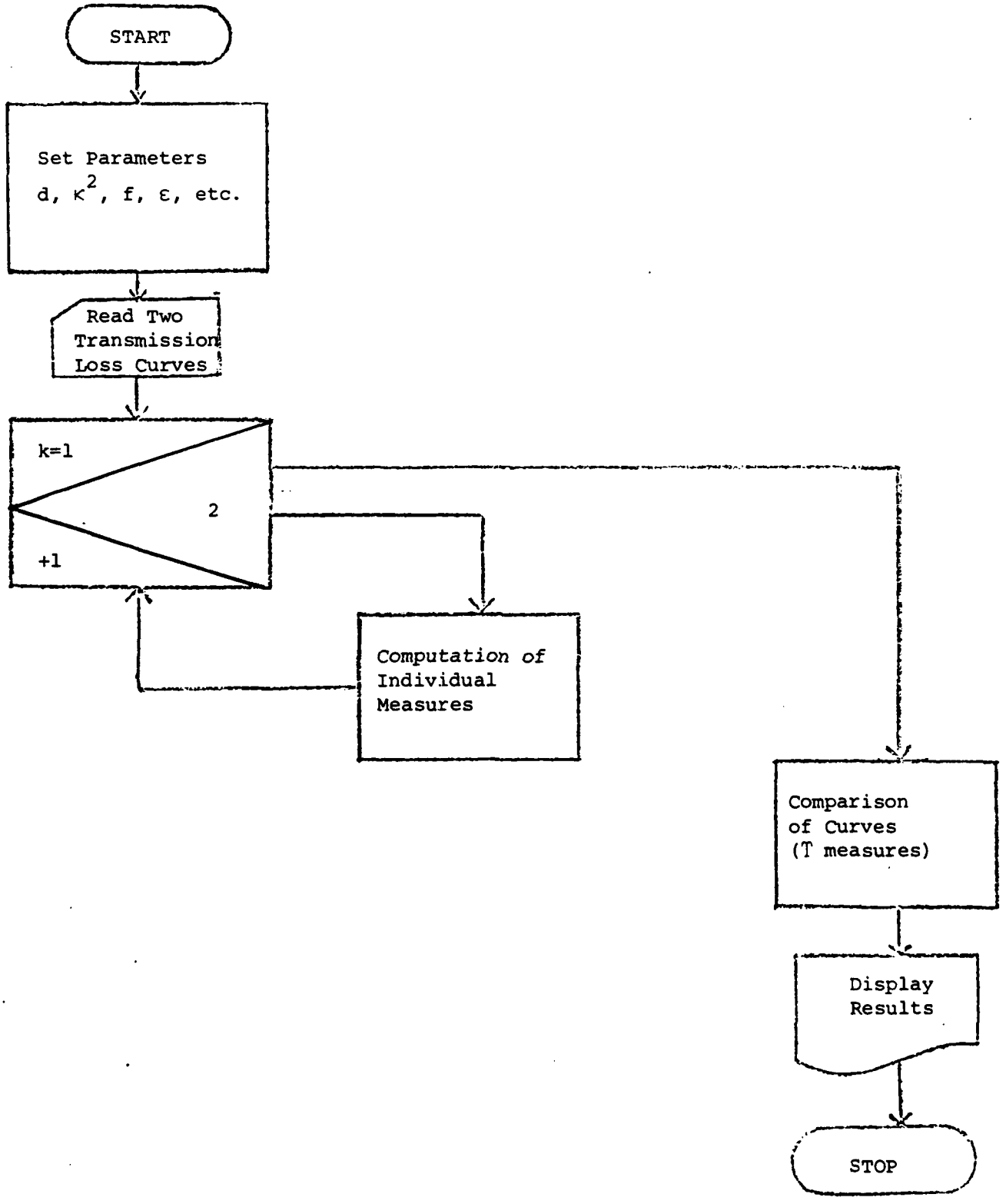


FIGURE 16. FUNCTIONAL FLOW OF SIMPLE MODEL FOR EXAMINING TWO PROPAGATION LOSS CURVES

## XI. Implementation Considerations

The next step in a process such as this is to implement enough of these tests (i.e., some or all of them) in order to allow them to be exercised against realistic transmission loss data of a variety of types. From such an exercise, meaningful values for the numerous parameters used in the measures (e.g., $\kappa^2$, f(r), $\gamma_1$, $\gamma_2$, $\varepsilon$ , d) should be obtained. Also, the analyst will acquire familiarity with the different measures and will see how different types of changes in the loss curves will affect the various measures. Only after such a period of analysis can one turn to "production use" of such measures. For a simplistic comparison program, one may quickly construct a program functionally similar to Fig. 16, but for flexibility and ease of later conversion to an operational model, one would probably desire something along the functional concept of Fig. 17. In each of these, the two functional boxes which now concern us are "Computation of Individual Measures" and "Comparison of Curves (T measures)": the remainder do not lie in the scope of this paper.

Under "Computation of Individual Measures" one would wish to compute $\ell_k$, $\theta_k$, $\chi_k$, $P_k$, $\Phi_k$, $R_{1,k}$, $\lambda_k$, $\Omega_{k,\infty}$ and $\Psi_k$. Now, the first two may be easily computed using the determinant minors of Appendix A, where trapozoidal integration is used for the quadrature. The third may be found by testing on a mesh. Then, the decision as to the existence of convergence zones is made (cf. Fig. 22). If there are no convergence zones, then the remaining quantities have no meaning, and the computation is complete. If there are convergence zones, the process continues. The mesh used for $T_k$ will also be used for $P_k$, and in most cases can be used for $\Phi_k$ as well. Both $P_k$ and $\Phi_k$ are computed in tabular form. The next two, $R_{1,k}$ and $\lambda_k$ are local maxima of functions, thus a common algorithm can be used for both of them. Of the various numeric algorithms available for a local maximum or minimum, a simple step search should form a more than

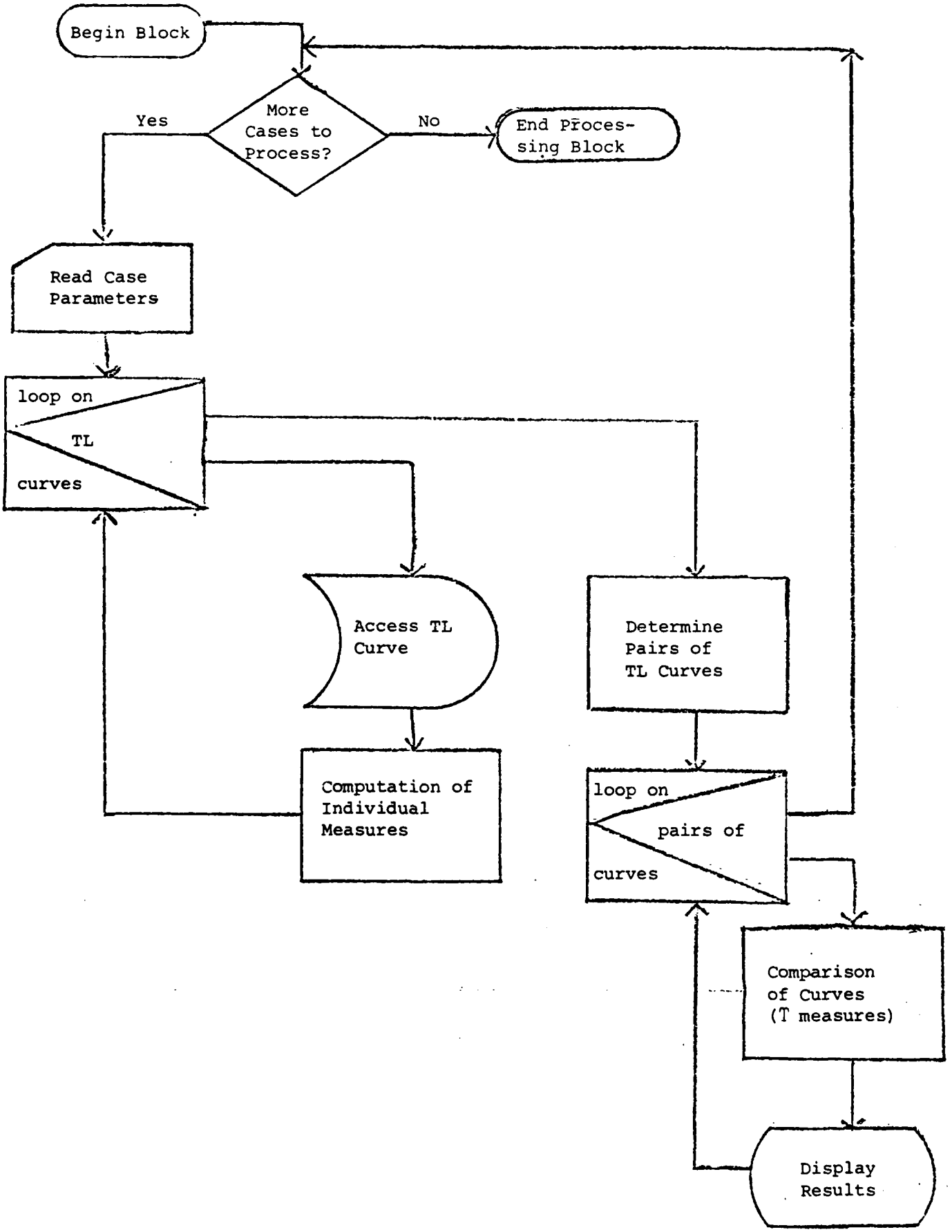


FIGURE 17. FUNCTIONAL FLOW OF MORE ADAPTABLE MODEL FOR COMPARISONS

adequate base for our algorithm. (Due to problems of multiple peaks, etc., several checks must be added to any "canned" algorithm before it is used on these functions.) The measure $\Omega_{k,\infty}$ may be found by numeric quadrature, and $\Psi_k$ may be obtained from the linear system given in Appendix Δ.

Under "Comparison of Curves" the measures $T_\alpha$ through $T_\kappa$ would be computed. There are ten types of measures, but since some measures are evaluated with different arguments ($T_\eta$, $T_\theta$, $T_\kappa$) there are thirteen scalar measures, and if one includes the linearly dependent $T_\kappa(3)$, there are fourteen scalar measures. The first seven ($T_\alpha$ through $T_\eta$) are computed from measures of the individual transmission loss curves (Ch. IX). Of these, $T_\alpha$ requires a quadrature; $T_\beta$, $T_\gamma$, $T_\delta$, $T_\varepsilon$, and $T_\zeta$ are computationally trivial; and, $T_\eta$ may be evaluated in closed form using the equations of App. E. The other three, detailed in Chapter X, require numeric quadrature. For $T_\theta$ and $T_\iota$ are not integrated in closed form, while $T_\kappa$ depends on $\Theta_{12}(\ell_{12})$, which in turn is obtained from a system of linear equations (App. A) whose coefficients were obtained by numeric quadrature.

Thus, it is seen that implementation of these measures is rather straightforward. And, if good use is made of subroutines to handle functions such as quadrature, solution of linear systems, determinants, and maxima/minima of functions, implementation should also be efficient.

## XII. Conclusions and Recommendations

The measures introduced in this report should give a good quantitative description of the characteristics discussed in Chapter III. However, there are a large number of parameters (e.g., constants, weighting functions) which must be determined by careful analysis. The heuristic values given for some of these are, as stated, merely estimates. Such an analysis would require these measures to be

computed for a wide selection of transmission loss curves, which implies a computer program of some kind to perform the myriad calculations. It is strongly suggested that such a computer-assisted analysis be performed as the next logical step towards an automated procedure for determining similarities and differences of transmission loss curves.

## APPENDIX A
## Estimation of $\ell_k$

The estimation of the minimizing functions $\ell_1$, $\ell_2$, and $\ell_{12}$ follows the standard methods of weighted least squares as developed in Ref. a and extended in Ref. b. However, the functionals $\Theta_1$, $\Theta_2$, and $\Theta_{12}$ are formed by integrals of rational functions of $T_k(r)$, and these functions are only specified at points. Therefore, before proceeding with the minimization, it is necessary to consider the effect of this tabular data.

Obviously, there is a large class of functions which will pass through the tabulated points; thus, there can be substantial variation in the resulting integrals. For most purposes, however, it may be assumed that the transmission loss curve can be modeled by "connecting the dots" of the tabulated data; i.e., linear interpolation.[38] In such a case, the integral of $T_k(r)$ is given exactly by the trapozoidal rule. That is, if $(x_i, T_k(x_i))$ are the range-transmission loss pairs, where

$$x_o = \delta$$

$$x_{i+1} = x_i + \Delta x$$

$$x_m = r_k$$

then

$$\int_\delta^{r_k} T_k(r)dr = \left\{\frac{1}{2} T_k(x_o) + \sum_{i=1}^{m-1} T_k(x_i) + \frac{1}{2} T_k(x_m)\right\} \Delta x$$

Now integrals of the form

$$\int_\delta^{r_k} T_k(r) f(r) dr$$

are not expressible exactly by the trapozoidal rule, for f(r) is not piecewise linear. The error involved, however, in applying the trapozoidal rule is small, and it is better to use this rule in such instances than to use either of Simpson's rules.

With the matter of quadrature methodology addressed, attention turns to the main problem. First, define four functions for the loss curve $T_k(r)$:

$$g_1^k(r) = 1$$

$$g_2^k(r) = \log r$$

$$g_3^k(r) = T_k(r)$$

$$g_4^k(r) = \alpha r$$

and define the determinant A(k) of integrals as

$$A(k) = |a_{ij}^k|_{4x4}$$

where

$$a_{ij}^k = \int_\delta^{r_k} g_i^k(r) g_j^k(r) f(r) dr$$

Or, expanding in detail,

$$a_{11}^k = \int_\delta^{r_k} f(r) dr$$

$$a_{12}^k = a_{21}^k = \int_\delta^{r_k} \log r \; f(r) dr$$

$$a_{13}^k = a_{31}^k = \int_\delta^{r_k} T_k(r) f(r) dr$$

$$a_{14}^k = a_{41}^k = \alpha \int_\delta^{r_k} r \; f(r) dr$$

$$a_{22}^k = \int_\delta^{r_k} \log^2 r \; f(r) dr$$

$$a_{23}^k = a_{32}^k = \int_\delta^{r_k} T_k(r) \log r \, f(r)dr$$

$$a_{24}^k = a_{42}^k = \alpha \int_\delta^{r_k} r \log r \, f(r)dr$$

$$a_{33}^k = \int_\delta^{r_k} T_k^2(r) f(r)dr$$

$$a_{34}^k = a_{43}^k = \alpha \int_\delta^{r_k} T_k(r) r \, f(r)dr$$

$$a_{44}^k = \alpha^2 \int_\delta^{r_k} r^2 f(r)dr$$

The coefficients $b_k$ and $\hat{b}_k$ of $\ell_k$ are given by the system

$$\begin{pmatrix} a_{11}^k & a_{12}^k \\ a_{21}^k & a_{22}^k \end{pmatrix} \begin{pmatrix} b_k \\ \hat{b}_k \end{pmatrix} = \begin{pmatrix} a_{13}^k & a_{14}^k \\ a_{23}^k & a_{24}^k \end{pmatrix} \begin{pmatrix} 1 \\ -1 \end{pmatrix}$$

Let $M_j^i(k)$ be the first minors of $A(k)$[39] and $M_{mn}^{ij}(k)$ the second minors.[40]

For notational convenience, let

$$N_{ij}(k) = M_{34}^{ij}(k)$$

Then

$$b_k = - \frac{N_{13}(k)+N_{14}(k)}{N_{34}(k)}$$

$$\hat{b}_k = - \frac{N_{23}(k)+N_{24}(k)}{N_{34}(k)}$$

and the minimum value of $\theta_k$ is

$$\frac{M_3^3(k) + M_4^3(k) + M_3^4(k) + M_4^4(k)}{a_{11}^k N_{34}(k)}$$

Direct application of the above yields $\ell_1$ and $\ell_2$. For $\ell_{12}$, define

$$a_{ij}^{12} = \frac{a_{ij}^1}{a_{11}^1} + \frac{a_{ij}^2}{a_{11}^2}$$

and use the above equations to get $b_{12}$, $\hat{b}_{12}$ and the minimum of $\Theta_{12}$.

## APPENDIX B

## On the Spacing of Convergence Zones

I. In order to formulate meaningful (yet hopefully simplistic) descriptors of the convergent zone placement, it is prudent to examine a reasonably realistic case for which the analytical solution is quite tractable. One may begin by using standard ray theory, which gives rise to caustics of infinite intensity. While such behavior is disastrous for propagation loss models, it is useful in this situation in that the peak of the convergence zone, or the caustic, is easily identified. By choosing a sound speed profile which is $C^2$, one eliminates the spurious caustics which sometimes arise in ray trace models (Ref. c).

II. Consider the analytic case with a range-independent parabolic profile

$$c(z) = c(z_o)/\{1-\gamma^2(z-z_o)^2\}^{1/2} \qquad \gamma > 0$$

where the sound axis is at depth $z_o$ and no depth is considered where

$$\gamma|z-z_o| \geq 1$$

Place the source on the sound axis, and for purposes of long-range calculation, only consider the refracted paths.[41] The ray paths are given by the equation.

$$z = z_o + \gamma^{-1}\sin\theta_o \sin\{\gamma x \sec\theta\}$$

$$\zeta = \gamma^{-1}\cos\theta_o\sin\{\gamma x \sec\theta_o\} + x \tan^2\theta_o \cos\{\gamma x \sec\theta_o\}$$

where $\theta_o$ is the initial tangent angle of the ray (Ref. c), and $\zeta$ is the partial derivative of z with respect to $\theta_o$ (Ref. d). Normally, $\zeta$ is used for the intensity calculation. The caustics will touch the ray paths at the zeros of $\zeta$; thus, the caustics will be given by the locus of points (x, z) on the ray paths for which $\zeta$ is zero. To simplify the analysis, the coordinate system will first be translated so that the origin is at the source, viz,

$$y = z - z_o$$

Then, the locus of (x, y) will be the caustic. The locus is given by

$$y = \gamma^{-1} \sin\theta_o \sin\{\gamma x \sec\theta_o\}$$

$$0 = \gamma^{-1} \cos\theta_o \sin\{\gamma x \sec\theta_o\} + x \tan^2\theta_o \cos\{\gamma x \sec\theta_o\}$$

The parameter $\theta_o$ is unwieldy, so transform the equations into a new parameter

$$\xi = \gamma x \sec\theta_o$$

to obtain

$$x = \frac{\xi}{\gamma} \sqrt{1 - \frac{1}{\xi} \tan\xi}$$

$$y = \frac{\sin\xi}{\gamma} \sqrt{1 - \xi\cot\xi}$$

For any value of $\xi$, in the following sequence of half-open intervals, there corresponds a (real) point on a caustic.

$$\xi \in ((m-1/2)\pi, m\pi]$$

$$m = 1, 2, 3, \ldots$$

The set of caustics is plotted in Fig. 18. This figure represents the entire caustic structure, which assumes that the only boundaries are the natural ones where $c(z)$ ceases to be defined [cf. the equation defining $c(z)$]. If attention is restricted to that range about the sound channel axis such that $c(z)$ is within 10% of $c(z_o)$, then the caustic structure appears as in Fig. 19, which has been scaled for visual purposes.

Now, consider the spacing between successive caustics along a horizontal cut. Along the sound channel axis the caustics have cusps (cf. Fig. 18) which are separated by $\pi/\gamma$. Along a horizontal cut which is not on the axis it is seen from Fig. 18 that the spacing is not constant, but in the region of interest to us (Fig. 19) it is nearly constant. To quantify this, the parameteric equations for the caustics are expanded about each cusp.

Writing

$$\xi = m\pi - \eta^2 \qquad m \epsilon Z^+$$

one may develop the power series

$$x = \frac{m\pi}{\gamma} - \frac{3}{2\gamma}\eta^2 + \frac{3}{8m\pi\gamma}\eta^4 - \frac{8m^2\pi^2-3}{48m^2\pi^2\gamma}\eta^6 + O(\eta^8)$$

$$y = \frac{1}{\gamma\sqrt{m\pi}}\eta^3 - \frac{1}{6\gamma(m\pi)^{3/2}}\eta^9 + O(\eta^{11})$$

In the vicinity of the cusp, the branch of the curve may be written (Bk. II, Ch. II of Ref. e) as

$$x = \frac{m\pi}{\gamma} - \frac{3}{2}\sqrt[3]{\frac{m\pi}{\gamma}}\, y^{2/3} + \frac{3}{8}\sqrt[3]{\frac{\gamma}{m\pi}}\, y^{4/3} + O(y^2)$$

Let $\Gamma$ denote the constant

$$\Gamma = \sqrt[3]{\frac{\pi}{\gamma}}$$

and consider the spacing between caustics of the transmission loss curve at constant depth

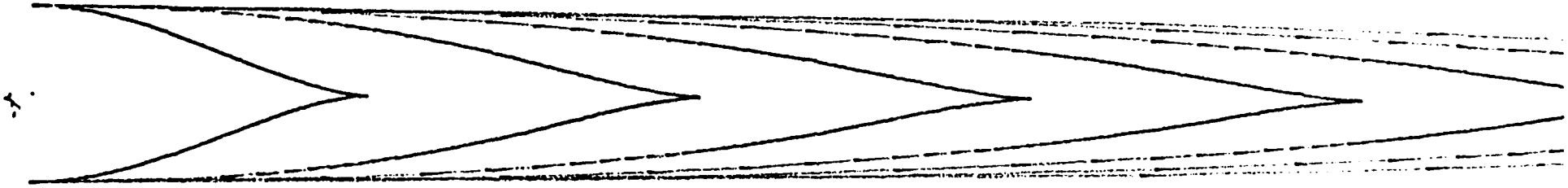

Figure 18. Caustics for Parabolic Profile, Natural Boundaries

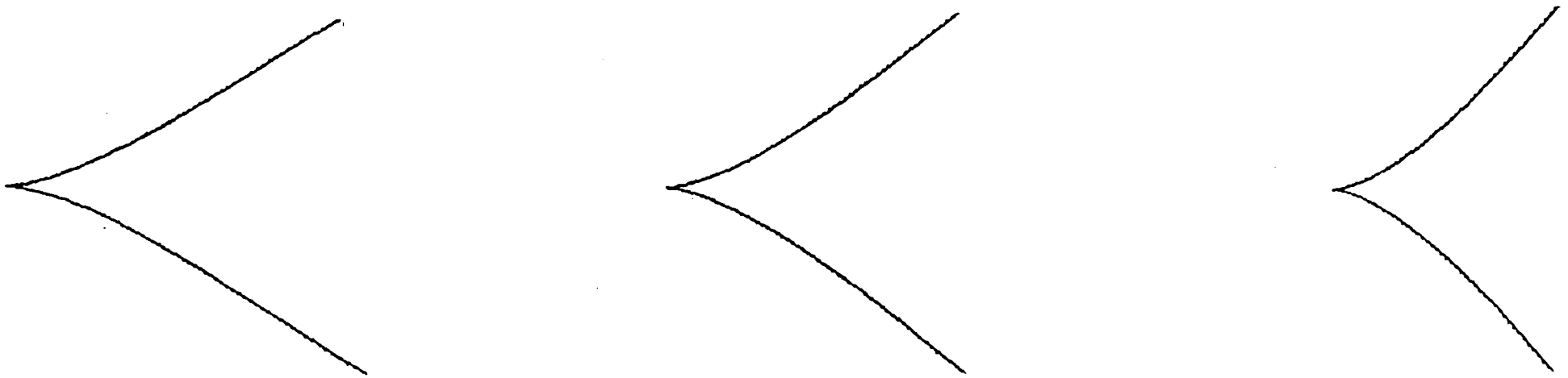

Figure 19. Caustics in the Vicinity of the Sound Channel Axis

$$z = z_o - \upsilon$$

for $\upsilon$ small in comparison with both the total depth and $1/\gamma$. Then, the spacing between the m-th and (m+1)st caustic at that depth is given by

$$\Delta_m x = \Gamma^3 - \frac{3}{2}\Gamma\left\{\sqrt[3]{m+1} - \sqrt[3]{m}\right\}\upsilon^{2/3} + \frac{3}{8}\Gamma^{-1}\left\{\frac{1}{\sqrt[3]{m+1}} - \frac{1}{\sqrt[3]{m}}\right\}\upsilon^{4/3}$$

$$+ O(\upsilon^2)$$

which may be approximated by

$$\Delta_m x \approx \Gamma^3 - \frac{1}{2}\Gamma m^{-2/3}\upsilon^{2/3} - \frac{1}{8}\Gamma^{-1} m^{-4/3}\upsilon^{4/3}$$

But, since

$$|\upsilon| << 1/\gamma$$

it is clear that $\Delta_m x$ is almost a constant.

III. Now consider a case where the source does not lie on the sound channel axis. Let the sound speed profile be the same as above, but place the source at range 0 and depth $z_1$ where

$$z_1 \neq z_o$$

Let $\theta_1$ be the tangent angle of the ray at the source, and let $\theta_o$ be the tangent angle of the ray path at the sound channel axis, so they are the ray angles at depths $z_1$ and $z_o$, respectively. Then

$$c(z_1)\ \sec\theta_1 = c(z_o)\ \sec\theta_o$$

The ray paths are given by

$$z = z_o + \gamma^{-1}\{\Xi\sin\{\gamma x \sec\theta_o\} - \gamma(z_0-z_1)\cos\{\gamma x \sec\theta_o\}\}$$

where

$$\Xi^2 = \sin^2\theta_o - \gamma^2(z_0-z_1)^2$$

so that

$$\frac{\partial\Xi}{\partial\theta_o} = \Xi^{-1}\sin\theta_o\cos\theta_o$$

and

$$\gamma\frac{\partial z}{\partial\theta_o} = \frac{\sin\theta_o\cos\theta_o}{\Xi}\sin\{\gamma x \sec\theta_o\} +$$

$$\Xi\,\gamma x \tan\theta_o \sec\theta_o \cos\{\gamma x \sec\theta_o\} +$$

$$\gamma(z_o-z_1)\gamma x \tan\theta_o \sec\theta_o \sin\{\gamma x \sec\theta_o\}$$

Now $d\theta_o/d\theta_1$ is non-vanishing for

$$|z_1-z_o| < 1/\gamma$$

so instead of setting $\zeta$ to zero, one may set[42]

$$\frac{\partial z}{\partial\theta_o} = 0$$

Making the transformation to the more tractable parameterization

$$\xi = \gamma x \sec\theta_o$$

$$\upsilon = z_0-z_1$$

$$y = z-z_0$$

which was used in the previous case, yields

$$\Xi^2 = 1 - \gamma^2\upsilon^2 - \gamma^2 x^2 \xi^{-2}$$

Since [43]

$$\sin\theta_o \neq 0$$

it may be divided out of the equation for the partial derivative, which then becomes (upon multiplication by $x\Xi$):

$$0 = x\cos\theta_o \sin\{\gamma x \sec\theta_o\} +$$

$$(z_0 - z_1)\gamma^2 x^2 \Xi \sec^2\theta_o \sin\{\gamma x \sec\theta_o\} +$$

$$\gamma x^2 \Xi^2 \sec^2\theta_o \cos\{\gamma x \sec\theta_o\}$$

or, in the new parameters,

$$\frac{\gamma x^2}{\xi}\sin\xi + \upsilon\xi^2\Xi\sin\xi + \gamma^{-1}\xi^2\Xi^2\cos\xi = 0$$

For notational simplicity, a number of $\beta_j$'s will be defined, starting with

$$\beta_1 = -\gamma^2\xi^{-2}$$

$$\beta_2 = 1 - \gamma^2\upsilon^2$$

Rationalizing the equation for x gives

$$(\gamma^4\sin^2\xi)x^4 + 2\gamma^2\xi^3\sin\xi\cos\xi(\beta_1 x^4 + \beta_2 x^2) + \xi^6\cos^2\xi(\beta_1^2 x^4 + 2\beta_1\beta_2 x^2 + \beta_2^2)$$

$$= \gamma^2\upsilon^2\xi^6\sin^2\xi(\beta_1 x^2 + \beta_2)$$

which may be written in powers of x as

$$\beta_3 + \beta_4 x^2 + \beta_5 x^4 = 0$$

where

$$\beta_3 = \xi^6 \beta_2{}^2 \cos^2\xi - \gamma^2 \upsilon^2 \xi^6 \beta_2 \sin^2\xi$$

$$\beta_4 = -2\gamma^2 \xi^3 \beta_2 \sin\xi\cos\xi + 2\beta_1 \beta_2 \xi^6 \cos^2\xi - \gamma^2 \upsilon^2 \xi^6 \beta_1 \sin^2\xi$$

$$\beta_5 = \gamma^4 \sin^2\xi + 2\beta_1 \gamma^2 \xi^3 \sin\xi\cos\xi + \beta_1{}^2 \xi^6 \cos^2\xi$$

or, in their factored form

$$\beta_3 = \xi^6 (1-\gamma^2\upsilon^2)(\cos^2\xi - \gamma^2\upsilon^2)$$

$$\beta_4 = \gamma^2 \xi^3 \{2\cos\xi(\sin\xi - \xi\cos\xi)(1- \gamma^2\upsilon^2) + \gamma^2\upsilon^2 \xi \sin^2\xi\}$$

$$\beta_5 = \gamma^4 (\sin\xi - \xi\cos\xi)^2$$

Now, make the change of variable

$$\psi = x^2 \gamma^2 \xi^{-3}$$

so the polynomial transforms into the quadratic

$$\beta_6 + \beta_7 \psi + \beta_8 \psi^2 = 0$$

where

$$\beta_6 = (1-\gamma^2\upsilon^2)(\cos^2\xi - \gamma^2\upsilon^2)$$

$$\beta_7 = 2\cos\xi(\sin\xi - \xi\cos\xi)(1-\gamma^2\upsilon^2) + \gamma^2\upsilon^2 \xi \sin^2\xi$$

$$\beta_8 = (\sin\xi - \xi\cos\xi)^2$$

This seems to be a rather simple formulation, and taking the discriminant, gives

$$\beta_7^2 - 4\beta_6\beta_8 = \{2\gamma\upsilon\sin\xi\}^2\beta_9^2$$

where

$$\beta_9^2 = \{1-\gamma^2\upsilon^2+\tfrac{1}{4}\gamma^2\upsilon^2\xi^2\}\sin^2\xi - \xi(1-\gamma^2\upsilon^2)\cos\xi\sin\xi$$

The roots of the quadratic are

$$\psi = \frac{-\beta_7 \pm 2\gamma\upsilon\beta_9\sin\xi}{2\beta_8}$$

Thus, to compute the caustics, one uses the parameter $\xi$, computes $\psi$, then $\Xi$, then x and y, remembering that most of the functions are multivalued,[44] i.e.,

$$\Xi = \sqrt{1-\gamma^2\upsilon^2-\xi\psi}$$

$$x = \gamma^{-1}\xi\sqrt{\xi\psi}$$

$$y = \gamma^{-1}\{\Xi\sin\xi-\gamma\upsilon\cos\xi\}$$

Now, for $\xi$ a positive integral multiple of $\pi$, there is a (real ) cusp on the caustic, which may be obtained by power series development. Let

$$\xi = m\pi - \eta^2 \qquad m\epsilon Z^+$$

then

$$\beta_6 = \beta_2^2-\beta_2\eta^4 + \frac{1}{3}\eta^8 - \frac{2}{45}\eta^{12} + O(\eta^{16})$$

$$\beta_7 = -2\pi m\beta_2 + \pi m(2-\gamma^2\upsilon^2)\eta^4 - \frac{1}{3}(2+\gamma^2\upsilon^2)\eta^6 - \frac{1}{3}\pi m(2-\gamma^2\upsilon^2)\eta^8 +$$

$$\frac{1}{15}(6-\gamma^2\upsilon^2)\eta^{10} + \frac{2\pi m}{45}(2-\gamma^2\upsilon^2)\eta^{12} + O(\eta^{14})$$

$$\beta_8 = \pi^2m^2 - \pi^2m^2\eta^4 + \frac{2\pi m}{3}\eta^6 + \frac{\pi^2m^2}{3}\eta^8 - \frac{2}{5}\pi m\eta^{10} + \frac{1}{45}(5-2\pi^2m^2)\eta^{12}$$

$$+ O(\eta^{14})$$

$$\beta_9 = \pi m(1-\gamma^2\upsilon^2)\eta^2 + \frac{1}{4}\gamma^2\pi^2m^2\upsilon^2\eta^4 + O(\eta^6)$$

$$\psi = \frac{\beta_2}{\pi m} + \frac{2\gamma\upsilon\sqrt{\beta_2}}{(\pi m)^{3/2}}\eta^3 - \frac{\gamma^2\upsilon^2}{2\pi m}\eta^4 + O(\eta^5)$$

$$x^2 = \frac{\pi^2m^2}{\gamma^2}\beta_2 - \frac{3\pi m\beta_2}{\gamma^2}\eta^2 + \frac{2(\pi m)^{3/2}\upsilon\sqrt{\beta_2}}{\gamma}\eta^3$$

$$+ \{3\gamma^{-2}\beta_2 - \frac{1}{2}m^2\pi^2\upsilon^2\}\eta^4 + O(\eta^5)$$

so the development of the curve about the cusp is

$$x = \sum_{j=0}^{\infty} w_{j1}\eta^j$$

$$y = \sum_{j=0}^{\infty} w_{j2}\eta^j$$

where

$$w_{01} = m\pi\gamma^{-1}\sqrt{\beta_2}$$

$$w_{02} = (-1)^{m+1}\upsilon$$

$$w_{11} = 0$$

$$w_{12} = 0$$

$$w_{21} = -\frac{3}{2}\gamma^{-1}\sqrt{\beta_2}$$

$$w_{22} = 0$$

$$w_{31} = \upsilon\sqrt{m\pi}$$

$$w_{32} = (-1)^m\gamma^{-1}\sqrt{\frac{5\beta_2}{m\pi}}$$

$$w_{41} = \frac{3\beta_2 - 2m^2\pi^2\gamma^2\upsilon^2}{8\gamma m\pi\sqrt{\beta_2}}$$

$$w_{42} = (-1)^m\frac{\upsilon}{2}$$

and so forth.

Thus, these cusps lie at uniform intervals in the range coordinate, but alternate in depths of $y=\pm\upsilon$. At one of the depths, there are cusps at a uniform spacing, but the caustic branches between the cusps are not equally spaced. But, since

$$|\upsilon| << 1/\gamma$$

and

$$\beta_2 \approx 1$$

the spacing is close to uniform.

IV. The final case to be considered is more realistic in that it has a surface boundary. Let the profile be parabolic, as before, with the channel axis at depth $z_o$, where

$$0 < z_o < 1/\gamma$$

As before, the depth coordinate is changed to

$$y = z - z_o$$

so that the source is at the origin, and let $\theta_o$ be the tangent angle at the source. Let

$$\Gamma_1 = \gamma^{-1}\cos\theta_o \ \mathrm{Arcsin}(\gamma z_o \cos\theta_o)$$

$$\Gamma_2 = 2\Gamma_1 + \gamma^{-1}\pi\cos\theta_o$$

$$\beta_{10}(x) = \left[\frac{x-\Gamma_1}{\Gamma_2}\right]$$

where [ ] is the greatest integer function. And, define the threshold

$$\overline{\theta}_o = \mathrm{Arcsin}(\gamma z_o)$$

Then, the ray paths have two forms, depending on whether they are refracted or surface reflected and refracted:

$$y = \gamma^{-1}\sin\theta_o \sin\{\gamma x \sec\theta_o\} \qquad |\theta_o| \le \overline{\theta}_o$$

$$y = \gamma^{-1}\sin\theta_o \sin\{\gamma(x-\beta_{10}(x)\Gamma_2)\sec\theta_o\} \qquad \overline{\theta}_o < |\theta_o| < \frac{\pi}{2}$$

Thus, the locus of caustics is described by two sets of equations, corresponding to the two cases above. In the first case, the caustic may be described by the same parametric equation used in the first case, except the domain of the parameter $\xi$ is different.

In the previous case, the domain was

$$\xi \in ((m-1/2)\pi, \ m\pi] \qquad m \in Z^+$$

But, in this case, the parametric equation for x yields

$$\gamma^2(1-\frac{1}{\xi}\tan\xi) = (\frac{\xi}{x})^2 = \frac{\gamma^2}{\cos^2\theta_o}$$

or

$$\xi\cot\xi + \cot^2\theta_o = 0$$

or

$$\xi\cot\xi + \cot^2\tilde{\theta}_o \leq 0$$

Let $\xi_m$ be the root of this equation between $(m-1/2)\pi$ and $m\pi$. Since in practice

$$z_o << 1/\gamma$$

the solutions are approximated by

$$\xi_m = m\pi\{1-\tan^2\bar{\theta}_o + \tan^4\bar{\theta}_o + (\frac{1}{3}m^2\pi^2 - 1)\tan^6\bar{\theta}_o$$

$$+(1-\frac{4}{3}m^2\pi^2)\tan^8\bar{\theta}_o - (\frac{1}{5}m^4\pi^4 - \frac{10}{3}m^2\pi^2 + 1)\tan^{10}\bar{\theta}_o\}$$

$$+ O(\tan^{14}\bar{\theta}_o)$$

And, the domain of the parameter is then

$$\xi\varepsilon(\xi_m, m\pi] \qquad\qquad m\varepsilon Z^+$$

Thus, along the sound channel axis are the cusps shown in Fig. 18.

Now, consider the caustic of the second part of the ray path family. Since interest will be restricted to the vicinity of the sound channel axis, it is sufficient to just consider those portions of the caustic which touch or cross the axis. This will require

$$y = 0$$

$$\frac{\partial y}{\partial \theta_o} = 0$$

simultaneously. But, from the second form, it is obvious that for

$$\theta_o \neq 0 \bmod \pi$$

these two cannot both be satisfied. Hence, along the sound channel axis, there is a series of equally spaced cusps on the caustic.

## APPENDIX Γ

## On the Choice of $\omega$

The short-span smoothing function $\omega_R(r)$ used in the calculation of $\Phi_k(R)$ must be defined before numeric compuations can be performed. Fortunately, there is a very wide latitude in the choice of such a function, and the final results are not very sensitive to the choice of function. Theoretically, one may choose $\omega_R(r)$ to be almost any $C_o^\infty$ function whose support was confined to a sufficiently small interval about R, say $[R-\varepsilon, R+\varepsilon]$. If $\omega_R(r)$ is $C_o^\infty$, then $\Phi_k(R)$ is $C^\infty$, and since

$$\text{supp } \omega_R \subset [R-\varepsilon, R+\varepsilon]$$

$\Phi_k(R)$ is $C_o^\infty$. In practice, however, $C_o^\infty$ functions generally do not lend themselves to rapid computation and one really does not need $\Phi_k(R)$ to be $C_o^\infty$, but merely $C^2$.

Thus, two possible forms for $\omega_R(r)$ are given, one reasonable (but not too good) and one excellent.

Form I: Choose constants $\gamma_1$, $\gamma_2$ where $\gamma_1$ is a dimensionless quantity greater than 1 and $\gamma_2$ is a positive distance (in miles), such that

$$\varepsilon = \gamma_2(\gamma_1-1)/\gamma_1$$

is a reasonable distance for integration. Then define

$$\gamma_3 = (\gamma_1-1)/\gamma_1$$

$$x = \frac{|R-r|}{\gamma_2}$$

$$\omega_R(r) = \begin{cases} \dfrac{\gamma_1 x + (1-\gamma_1)}{x-1} & \text{if } x < \gamma_3 \\ 0 & \text{if } x \geq \gamma_3 \end{cases}$$

$$\tilde{\omega}_R(r) = \begin{cases} \dfrac{1}{\gamma_2 (x-1)^2} & \text{if } x < \gamma_3 \text{ and } R \leq r \\ -\dfrac{1}{\gamma_2 (x-1)^2} & \text{if } x < \gamma_3 \text{ and } R > r \\ 0 & \text{if } x \geq \gamma_3 \end{cases}$$

$$\tilde{\tilde{\omega}}_R(r) = \begin{cases} -\dfrac{2}{\gamma_2^2 (x-1)^3} & \text{if } x < \gamma_3 \text{ and } R \leq r \\ \dfrac{2}{\gamma_2^2 (x-1)^3} & \text{if } x < \gamma_3 \text{ and } R > r \\ 0 & \text{if } x \geq \gamma_3 \end{cases}$$

Then, the supports of the functions are intervals of width $2\varepsilon$, i.e.

$$\text{supp } \omega_R = [R-\varepsilon,\ R+\varepsilon]$$

$$\text{supp } \tilde{\omega}_R = [R-\varepsilon,\ R+\varepsilon]$$

$$\text{supp } \tilde{\tilde{\omega}}_R = [R-\varepsilon,\ R+\varepsilon]$$

Also

$$\frac{\partial \omega_R(r)}{\partial R} = \tilde{\omega}_R(r)$$

and

$$\frac{\partial^2 \omega_R(r)}{\partial R^2} = \tilde{\tilde{\omega}}_R(r)$$

except at the three points

$$r = R - \varepsilon$$

$$r = R$$

$$r = R + \varepsilon$$

where the left- and right-hand first partials exist, but are not equal, and no second partials exist.

A reasonable set of values is

$$\gamma_1 = 2$$

$$\gamma_2 = 8 \text{ nm.}$$

which gives

$$\varepsilon = 4 \text{ nm.}$$

$$x = \frac{1}{8} |R-r|$$

$$\omega_R(r) = \max(0, \frac{2x-1}{x-1})$$

Then

$$\Phi_k'(R) \stackrel{d}{=} \frac{d\Phi_k(R)}{dR} = \int_\delta^{r_k} P_k(r)\tilde{\omega}_R(r)f(r)dr$$

$$\Phi_k''(R) \stackrel{d}{=} \frac{d^2\Phi_k(R)}{dR^2} = \int_\delta^{r_k} P_k(r)\tilde{\tilde{\omega}}_R(r)f(r)dr$$

$$+ \frac{1}{4}\{P_k(R-4)f(R-4)I_{[\delta,r_k]}(R-4)$$

$$+P_k(R+4)f(R+4)I_{[\delta,r_k]}(R+4)\}$$

$$- \frac{1}{16} P_k(R)f(R)I_{[\delta,r_k]}(R)$$

where I is the indicator function, viz

$$I_A(r) = \begin{cases} 0, & \text{if } r \notin A \\ 1, & \text{if } r \in A \end{cases}$$

Now, since P is continuous (though not differentiable), $\Phi_k(R)$ is $C^2$, but the rather jagged form of $T_k(r)$ may give $\Phi_k''(R)$ a very large Total Variation which has some undesirable, but not fatal, side effects in terms of computer implementation.

Form II. Choose a constant $\gamma_2$ to be a positive distance, in nm., such that $\varepsilon = \pi\gamma_2$ is a small number of miles (e.g., 4 nm.). Define

$$x = \frac{R-r}{\gamma_2}$$

$$\omega_R(r) = \begin{cases} 1 + \cos x & |x| < \pi \\ 0 & |x| > \pi \end{cases}$$

$$\tilde{\omega}_R(r) = \begin{cases} -\frac{1}{\gamma_2} \sin x & |x| < \pi \\ 0 & |x| \geq \pi \end{cases}$$

$$\tilde{\tilde{\omega}}_R(r) = \begin{cases} -\frac{1}{\gamma_2^2} \cos x & |x| < \pi \\ 0 & |x| \geq \pi \end{cases}$$

Then

$$\frac{\partial \omega_R(r)}{\partial R} = \tilde{\omega}_R(r)$$

at all points

$$\frac{\partial^2 \omega_R(r)}{\partial R^2} = \tilde{\tilde{\omega}}(r)$$

except at $r = R \pm \varepsilon$, where left- and right-hand second partials exist, but are not equal. In this case, we have

$$\Phi_k'(R) = \int_\delta^{r_k} P_k(r)\tilde{\omega}_R(r)f(r)dr$$

$$\Phi_k''(R) = \int_\delta^{r_k} P_k(r)\tilde{\tilde{\omega}}_R(r)f(r)dr$$

This form for $\omega$ gives rise to a much smoother $\Phi_k''(R)$ (indeed, it is even $C^1$), which will not have the problems that can arise with the previous form.

## Appendix Δ
## Estimation of $\Phi_k$.

The shape of the transmission loss curve $T_k$ about $R_j$ was modelled using the form

$$\Psi_k(r) = \begin{cases} d_1 + d_2 x + \dfrac{d_3}{x+d_o} & r \geq R_j \\ d_4 + d_5 x + \dfrac{d_6}{x-d_o} & r < R_j \end{cases}$$

Since the monotonic component should not affect the coefficients of the shape function, $\Psi_k(r)$ will be fit to the perturbation rather than the loss curve itself. But $P_k(r)$ may be quite rough (cf. Fig. 8); thus, rather than fit the smooth curve $\Psi_k(r)$ to $P_k(r)$, it will be fit to $\Phi_k(r)$, the smoothed perturbation function.

The form for $\Psi_k$ was chosen so that a variety of shapes common to convergence zone peaks could be accommodated. In this, however, the parameter $d_o$ should not be estimated, but should be chosen beforehand. This ensures that when one is comparing different transmission loss curves $T_1$ and $T_2$, then the examination of the convergence zone shapes, $\Psi_1$ and $\Psi_2$, can be easily accomplished. For if $d_o$ were different for $\Psi_1$ and $\Psi_2$, meaningful comparison would be very difficult. Thus, $d_o$ will be a chosen constant, say 5 nm. (this may be adjusted when implemented). Furthermore, $\Psi_k$ should be $C^1$, but not necessarily $C^2$. Thus, one has

$$d_1 + d_3/d_o = d_4 - d_6/d_o$$

$$d_2 - d_3/d_o^2 = d_5 - d_6/d_o^2$$

The first equation is the condition that $\Psi_k(r)$ be continuous at $R_j$, the second equation is the condition that $\Psi_k'(r)$ be continuous at $R_j$. These may be rewritten as

$$d_3 - d_6 = d_o^2(d_2-d_5)$$

$$d_3 + d_6 = d_o(d_4-d_1)$$

Now, let $\hat{\omega}_R(r)$ be a weighting function (as developed in App. Γ), which need not be identical with $\omega_R(r)$. This new weighting function is to allow the fit to be made in the vicinity of the convergenze zone, and allows for situations such as Fig. 20 where the zone shapes are the same, but their size is different. For this type of fit, a weighting function of Form I (cf. App. Γ) is superior to one of Form II.

We then wish to choose the coefficient of $\Psi_k$ to minimize the form

$$\Pi = \int_{\delta}^{r_k} \hat{\omega}_{Rj}(r)[\Phi_k(r)-\Psi_k(r)]^2 dr$$

This may be quickly done using Lagrangian multipliers, by forming

$$\frac{1}{2}\Pi + d_7[d_3+d_6+d_o(d_1-d_4)] + d_8[d_3-d_6-d_o^2(d_2-d_5)]$$

where $d_7$ and $d_8$ are the multipliers. Then, define the functions

$$e_1 = 1$$

$$e_2 = r-R_j$$

$$e_3 = (r-R_j+d_o)^{-1}$$

$$e_4 = \Phi_k(r)$$

and the integrals

$$J_{pq} = \int_{\delta}^{R_j} \omega_{R_j}(r) e_p e_q dr$$

$$\tilde{J}_{pq} = \int_{R_j}^{r_k} \omega_{R_j}(r) e_p e_q dr$$

Define the column vectors

$$D = \begin{bmatrix} d_1 \\ d_2 \\ \vdots \\ d_8 \end{bmatrix} \qquad F = \begin{bmatrix} J_{14} \\ J_{24} \\ J_{34} \\ \tilde{J}_{14} \\ \tilde{J}_{24} \\ \tilde{J}_{34} \\ o \\ o \end{bmatrix}$$

and the 8x8 symmetric matrix

$$H = \left[\begin{array}{ccc|ccc|cc} J_{11} & J_{12} & J_{13} & O & O & O & d_o & O \\ J_{21} & J_{22} & J_{23} & O & O & O & O & -d_o^2 \\ J_{31} & J_{32} & J_{33} & O & O & O & 1 & 1 \\ \hline O & O & O & \tilde{J}_{11} & \tilde{J}_{12} & \tilde{J}_{13} & -d_o & O \\ O & O & O & \tilde{J}_{21} & \tilde{J}_{22} & \tilde{J}_{23} & O & d_o^2 \\ O & O & O & \tilde{J}_{31} & \tilde{J}_{32} & \tilde{J}_{33} & 1 & -1 \\ \hline d_o & O & 1 & -d_o & O & 1 & O & O \\ O & -d_o^2 & 1 & O & d_o^2 & -1 & O & O \end{array}\right]$$

Then, the vector D which minimizes the form is given by the linear system

$$HD = F .$$

Figure 20. Transmission loss curves with same shape convergence zones, but different structures.

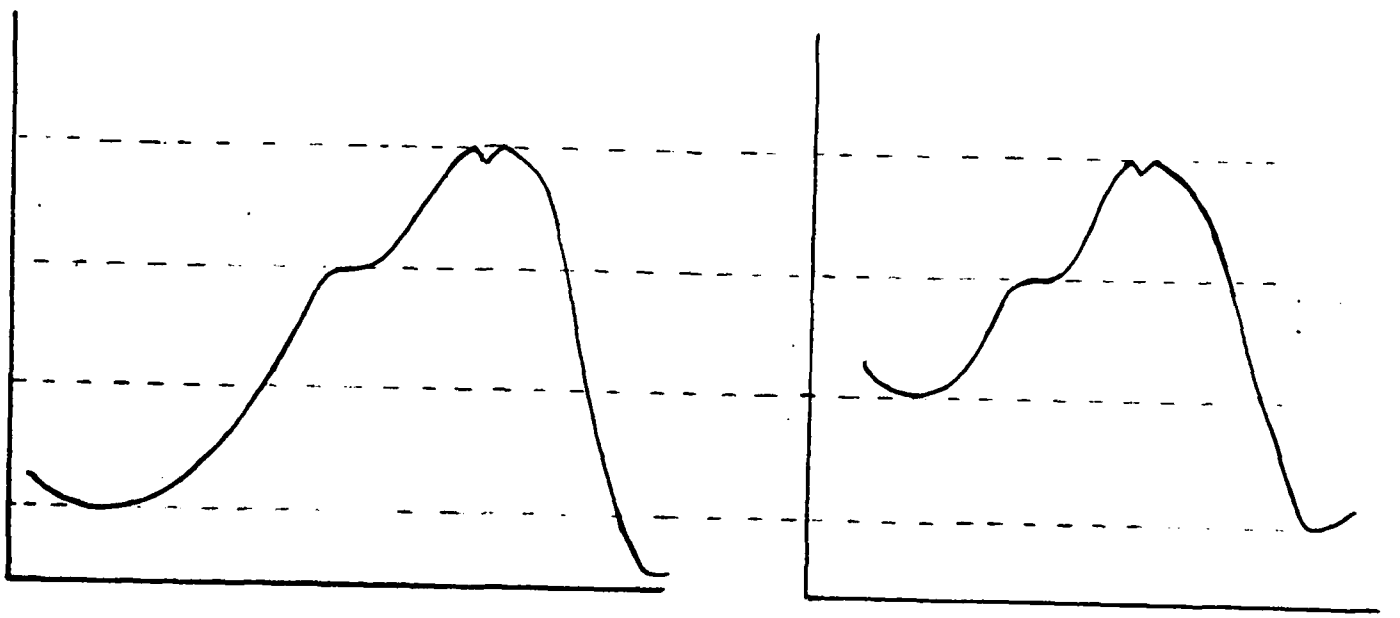

By inspection, one may reduce this to a 4x4 system, but the previous form has advantages (it is a symmetric bordered block diagonal matrix). For this curve fit to be geometrically meaningful, one should have

$$d_2 < 0$$

$$d_5 > 0$$

If either of these conditions is not met by the solution vector D, then the convergence zone has a shape which is not amenable to this type of fit, and the D vector should not be used.

## Appendix E
## Evaluation of $T_\eta$

In this appendix, the problem of computing

$$T_\eta(j) = \min_{\phi} \frac{\int_{-\infty}^{\infty} \hat{\omega}_o(x)\,(\Psi_1(x+R_{j1}) - \Psi_2(x+R_{j2}) + \phi)^2 dx}{\int_{-\infty}^{\infty} \hat{\omega}_o(x)\,dx}$$

will be considered. For notational convenience, let

$$E_q^+ = \int_0^{\infty} \hat{\omega}_o(x)\,(\Psi_1(x+R_{j1}) - \Psi_2(x+R_{j2}))^q dx$$

$$E_q^- = \int_{-\infty}^{0} \hat{\omega}_o(x)\,(\Psi_1(x+R_{j1}) - \Psi_2(x+R_{j2}))^q dx$$

$$E_q = E_q^- + E_q^+$$

for

$$q = 0,\ 1,\ 2$$

Using standard techniques, the minimum occurs when

$$\phi = -E_1/E_0$$

and is

$$T_\eta(j) = \{E_2E_0 - E_1^2\}/E_0^2$$

where the E's are, of course, dependent upon the index j.

$$E_1^- = \gamma_2\gamma_3\{h_4\gamma_1 - \tfrac{1}{2}\gamma_2(\gamma_1+1)h_5\}$$

$$- \frac{h_6}{d_o+\gamma_2}\{\gamma_1 d_o+\gamma_1\gamma_2-\gamma_2\}\{\ell n(\gamma_2\gamma_3+d_o)-\ell n\ d_o\}$$

$$+ \frac{\gamma_2}{d_o+\gamma_2}\{(-h_4+\gamma_2 h_5)(d_o+\gamma_2)+h_6\}\ell n\gamma_1$$

$$E_2^+ = \int_o^{\varepsilon}\{\gamma_1 h_1^2+2\gamma_1 h_1 h_2 x + \frac{2\gamma_1 h_1 h_3}{x+d_o} + \gamma_1 h_2^2 x^2 + \frac{2\gamma_1 h_2 h_3 x}{x+d_o}$$

$$+ \frac{\gamma_1 h_3^2}{(x+d_o)^2} + \frac{\gamma_2 h_1^2}{x-\gamma_2} + \frac{2\gamma_2 h_1 h_2 x}{x-\gamma_2} + \frac{2\gamma_2 h_1 h_3}{(x+d_o)(x-\gamma_2)}$$

$$+ \gamma_2 h_2^2\{x+\gamma_2 + \frac{\gamma_2^2}{x-\gamma_2}\} + \frac{2\gamma_2 h_2 h_3 x}{(x+d_o)(x-\gamma_2)} + \frac{\gamma_2 h_3^2}{(x+d_o)^2(x-\gamma_2)}\}dx$$

$$= \gamma_1\gamma_2\gamma_3\ h_1^2 + \gamma_1\gamma_2^2\gamma_3^2 h_1 h_2 + 2\gamma_1 h_1 h_3\{\ell n(\gamma_2\gamma_3+d_o)-\ell n\ d_o\}$$

$$+ \tfrac{1}{3}\gamma_1\gamma_2^3\gamma_3^3 h_2^2 + 2\gamma_1 h_2 h_3\{\gamma_2\gamma_3 - d_o\ \ell n(\gamma_2\gamma_3+d_o) + d_o\ \ell n\ d_o\}$$

$$+ \frac{\gamma_1\gamma_2\gamma_3 h_3^2}{d_o(\gamma_2\gamma_3+d_o)} - \gamma_2 h_1^2 \ell n\ \gamma_1 + 2\gamma_2^2 h_1 h_2\{\gamma_3 - \ell n\gamma_1\}$$

$$+ \frac{2\gamma_2 h_1 h_3}{\gamma_2+d_o}\{\ell n\ d_o - \ell n(\gamma_2\gamma_3+d_o) - \ell n\gamma_1\} + \gamma_2^3 h_2^2\{\tfrac{1}{2}\gamma_3^2+\gamma_3-\ell n\gamma_1\}$$

$$+ \frac{2\gamma_2 h_2 h_3}{\gamma_2+d_o}\{d_o\ell n(\gamma_2\gamma_3+d_o) - d_o\ \ell n\ d_o - \gamma_2\ \ell n\ \gamma_1\}$$

$$+ \frac{\gamma_2 h_3^2}{(\gamma_2+d_o)^2}\left|\frac{d_o+\gamma_2}{d_o+\gamma_2\gamma_3} - \frac{d_o+\gamma_2}{d_o} + \ell n\ d_o - \ell n(\gamma_2\gamma_3+d_o)-\ell n\gamma_1\right|$$

$$= (\gamma_1-1)\gamma_2\left|h_1^2+\gamma_2\gamma_3 h_1 h_2 + \tfrac{1}{3}\gamma_2^2\gamma_3^2 h_2^2 + 2h_2 h_3 + \frac{h_3^2}{d_o(\gamma_2\gamma_3+d_o)}\right|$$

If $\hat{\omega}_R(r)$ has Form I of Appendix Γ (which is the preferred form for this function, cf. App.Γ), then one has (reiterating App.Γ)

$$\hat{\omega}_o(x) = \gamma_1 + 1/\{-1+|x|/\gamma_2\}$$

$$\gamma_3 = 1 - 1/\gamma_1$$

$$\varepsilon = \gamma_2\gamma_3 > 0$$

Let $h_i$ be the difference of the $d_i$'s for the j-th peak two transmission loss curves, i.e.,

$$h_i = d_i(1) - d_i(2) \qquad i = 1, 2, 3, 4, 5, 6$$

where $d_i(k)$ is $d_i$ of $T_k(r)$ at $R_j$.

The evaluation of the integrals is straight-forward.

$$E_0^+ = \int_o^\varepsilon (\gamma_1 + \frac{\gamma_2}{x-\gamma_2})dx = \gamma_1\gamma_2\gamma_3 - \gamma_2 \ell n\gamma_1$$

$$E_0^- = E_0^+$$

$$E_1^+ = \int_o^\varepsilon \{\gamma_1 h_1 + \gamma_2 h_2 x + \frac{\gamma_1 h_3}{x+d_o} + \frac{\gamma_2 h_1}{x-\gamma_2} + \frac{\gamma_2 h_2 x}{x-\gamma_2} + \frac{\gamma_2 h_3}{(x+d_o)(x-\gamma_2)}\}dx$$

$$= \gamma_1\gamma_2\gamma_3 h_1 + \frac{1}{2}\gamma_1\gamma_2^2\gamma_3^2 h_2 + \gamma_1 h_3\{\ell n(\gamma_2\gamma_3+d_o) - \ell n\, d_o\}$$

$$- \gamma_2 h_1 \ell n\gamma_1 + \gamma_2^2 h_2\{\gamma_3 - \ell n\gamma_1\} + \frac{\gamma_2 h_3}{d_o+\gamma_2}\{\ell n\, d_o - \ell n(\gamma_2\gamma_3+d_o) - \ell n\gamma_1\}$$

$$= \gamma_2\gamma_3\{h_1\gamma_1 + \frac{1}{2}\gamma_2(\gamma_1+1)h_2\}$$

$$+ \frac{h_3}{d_o+\gamma_2}\{\gamma_1 d_o + \gamma_1\gamma_2 - \gamma_2\}\{\ell n(\gamma_2\gamma_3+d_o) - \ell n\, d_o\}$$

$$- \frac{\gamma_2}{d_o+\gamma_2}\{(h_1+\gamma_2 h_2)(d_o+\gamma_2)+h_3\}\ell n\gamma_1$$

$$+ \gamma_2^2\gamma_3 \left\{\frac{1}{2}\gamma_2(\gamma_3+2)h_2^2 + 2h_1h_2 - \frac{h_3^2}{d_o(\gamma_2+d_o)(\gamma_2\gamma_3+d_o)}\right\}$$

$$+\{2(\gamma_2(\gamma_1-1) + \gamma_1 d_o)(h_1-d_o h_2)(\gamma_2+d_o) - \gamma_2 h_3\} \frac{h_3}{(\gamma_2+d_o)^2}$$

$$\cdot \{\ell n(\gamma_2\gamma_3+d_o) - \ell_n\, d_o\}$$

$$- \gamma_2\left\{h_1 + \gamma_2 h_2 + \frac{h_3}{\gamma_2+d_o}\right\}^2 \ell n\gamma_1$$

$$E_2^- = (\gamma_1-1)\gamma_2 \left\{h_4^2 - \gamma_2\gamma_3 h_4 h_5 + \frac{1}{3}\gamma_2^2\gamma_3^2 h_5^2 + 2h_5h_6 + \frac{h_6^2}{d_o(\gamma_2\gamma_3+d_o)}\right\}$$

$$+ \gamma_2^2\gamma_3 \left\{\frac{1}{2}\gamma_2(\gamma_3+2)h_5^2 - 2h_4h_5 - \frac{h_6^2}{d_o(\gamma_2+d_o)(\gamma_2\gamma_3+d_o)}\right\}$$

$$- \{2(\gamma_2(\gamma_1-1) + \gamma_1 d_o)(h_4+d_o h_5)(\gamma_2+d_o) + \gamma_2 h_6\} \frac{h_6}{(\gamma_2+d_o)^2}$$

$$\cdot \{\ell n(\gamma_2\gamma_3 + d_o) - \ell n\, d_o\}$$

$$- \gamma_2 \left\{h_4 - \gamma_2 h_5 - \frac{h_6}{\gamma_2+d_o}\right\}^2 \ell n\gamma_1$$

From these terms $T_\eta(j)$ may easily be computed.

## Notation

Since a number of different mathematical symbols are used in this paper, this list of notation and variables is given for convenient reference.

| | |
|---|---|
| $\stackrel{d}{=}$ | is defined to be equal to |
| $\equiv$ | is identically equal to |
| $\not\equiv$ | is not congruent to |
| $[a,b]$ | the closed interval from a to b |
| $(0,\infty)$ | the open interval from zero to infinity |
| $\min_{\phi}$ | the minimum over all values of $\phi$ of the function. |
| $\|\|.\|\|_p$ | $L_p$ norm |
| supp | support of the function |
| log | common logarithm |
| ln | natural logarithm |
| $\lim_{x \downarrow o}$ | limit as x decreases to zero |
| fog | composition of functions |
| $\cap$ | intersection of sets |
| $\epsilon$ | is an element of |
| $O(\eta)$ | a function such that $O(\eta)/\eta$ is bounded as $\eta$ goes to zero |
| mod | modulo |

## Latin Notation

| | |
|---|---|
| A(k) | determinent used to obtain monotonic component of $T_k$, defined in App. A. |
| $a_{ij}^k$ | element of A(k), defined in App. A |

| | |
|---|---|
| $b_k, \hat{b}_k$ | coefficients of $\ell_k$, defined in App. A |
| $C^1, C^2, C_*^\infty$ | spaces of continuous curves |
| $c(z)$ | sound speed profile, used in App. B |
| $D$ | column vector used in App. $\Delta$ |
| $d_j$ | coefficients of shape function $\Psi_k$ |
| $E_q, E_q^+, E_q^-$ | integrals of polynomials in the $\Psi_k$, defined in App. E |
| $\hat{E}_q$ | integrals of polynomials in the $G_j$ functions, defined in Ch.X. |
| $e_j$ | functions used as integrand factors in App. $\Delta$ |
| $F$ | column vector of integrals, used in determination of $\Psi_k$, defined in App. $\Delta$ |
| $f(r)$ | weighting function for integrals, defined in Chap. IV |
| $G_k(v)$ | scaled form of the perturbation function, defined in Ch.X |
| $g_j^k$ | functions used as factors in integrals, defined in App. A |
| $H$ | symmetric matrix of linear system, defined in App. $\Delta$ |
| $h_i$ | differences in the coefficients of the two $\Psi_k$'s, defined in App. E. |
| $I_A(r)$ | indicator function for set A with argument r, used in App. $\Gamma$ |
| $i_o$ | index optimizing $T_\delta$, defined in Ch. IX |
| $J_{pq}$, $\tilde{J}_{pq}$ | integrals used in the matrix H and vector F, defined in App. $\Delta$ |
| $j_o$ | index optimizing $T_\delta$, defined in Ch. IX |
| $k$ | index of transmission loss function |
| $L_p$ | $L_p$ norm of function, defined in Ch. II |
| $\ell_k$ | montonic component of loss function, cf. App. A |

| | |
|---|---|
| $M^i_j(k)$ | first order minor of A(k), used in App. A. |
| $M^{ij}_{mn}(k)$ | second order minor of A(k), used in App. A. |
| m | index of caustic, used in App. B. |
| $N_{ij}(k)$ | abbreviated minor of A(k), defined in App. A. |
| $P_k$ | perturbation component of $T_k$, defined in Ch. IV. |
| $P_{kk}$ | perturbation component of $T_k$ with respect to $\ell_{12}$. |
| p | norm value used for $T_\theta$ |
| $\tilde{p}$ | parameter used in defining $\chi_k$ |
| $Q_\lambda(r)$ | function used to determine spacing of sucessive convergence zones, defined in Ch. VII. |
| $R_o$ | parameter used in locating first convergence zone |
| $R_1, R_{1,k}$ | distance from source to first convergence zone (actually, to the first peak of $P_k$ which may or may not be the first convergence zone) |
| $R_j$ | distance from source to $j^{th}$ peak of $P_k$ |
| $r_k$ | maximum range of tabulated data for $k^{th}$ transmission loss curve |
| $r_{12}$ | maximum common range of transmission loss curves |
| s | lower limit of integration, used in Ch. IX |
| $T_k(r)$ | $k^{th}$ transmission loss function |
| t | upper limit of integration, used in Ch. IX |
| $[t_1, t_2]$ | intersections of domains in uniform range space, defined in Ch.X |
| $V_k$ | linear transformation mapping first two peaks of $P_k$ into 0 to 1 respectively, defined in Ch. X |
| v | argument in uniform range space, used in Ch. X |
| $w_{ij}$ | Taylor series expansion coefficients, defined in App. B |

| | |
|---|---|
| $x$ | general variable used for range, particularly for caustic calculation, cf. App. B |
| $y$ | depth, measured from sound channel axis, used in App. B |
| $z^+$ | the positive integers $\langle 1,2,3,\ldots \rangle$ |
| $z, z_o, z_1$ | depths for use with sound speed profiles, cf. App. B |

Greek Notation

| | |
|---|---|
| $\alpha$ | attenuation coefficient |
| $\beta_j$ | variables of convience, used in second case in App. B |
| $\Gamma$ | constant used in App. B |
| $\gamma_j$ | coefficients used in representations of $\omega$ and $\tilde{\omega}$ functions, defined in App. $\Gamma$ |
| $\gamma$ | parameter of parabolic sound speed profile, used in App. B |
| $\Delta_j$ | foward difference operator |
| $\delta$ | minimum range of tabulated transmission loss curves, defined in Ch. IV |
| $\epsilon$ | parameter related to support of $\omega$, defined in App. $\Gamma$ |
| $\tilde{\epsilon}_j$ | perturbation component for convergence zone spacing |
| $\zeta$ | derivative whose zeros identify caustics, defined in App. B. |
| $\zeta_k(v)$ | scaled weighting function for uniform range space, defined in Ch. X |
| $\eta$ | infinitesmal used in development of power series for caustics, defined in App. B |
| $\theta_k, \theta_{12}$ | minimization functionals for monotonic components, defined in Ch. V |
| $\theta_o, \theta_1$ | angle of raypath at depths $z_o$ and $z_1$ for caustic calculations, used in App B |
| $\tilde{\theta}$ | threshold for $\chi_k$, used in Ch. VI |
| $\kappa, \tilde{\kappa}$ | thresholds for tests dealing with existance of convergence zones, used in Ch. VI |

| | |
|---|---|
| $\Lambda$ | 'average' distance between convergence zones |
| $\lambda_k$ | estimate of $\Lambda$ for $k^{th}$ transmission loss curve |
| $\mu$ | geometric mean, used in Ch. IV |
| $\Xi$ | form used in raypath and caustic calculations for second case in App. B |
| $\xi$ | used in parameterization of caustic curves, defined in App. B. |
| $\xi_m$ | roots of a transendental equation used for caustics, defined in App. B |
| $\Pi$ | optimization functional for $\Psi_k$, defined in App. $\Delta$ |
| $\pi$ | constant |
| $\rho$ | upper limit of integration for a candidate measure, used in Ch. X |
| $\tilde{\sigma}$ | threshold for $\sigma_k$, used in Ch. VI |
| $\sigma_k$ | optimizing value of parameter $\sigma$ for $\chi_k$, defined in Ch. V |
| $\tau$ | shift parameter in candidate measure, used in Ch. X |
| $T_\alpha$,etc | measures relating to the similarities of the two transmission loss curves |
| $\upsilon$ | parameter for depth, used in App. B |
| $\Phi_k$ | smoothed perturbation function |
| $\phi$ | minimization variable used in functionals |
| $\Psi_k$ | function used for describing shape of peak, defined in Ch. VIII |
| $\psi$ | transformation variable used in App. B |
| $\chi_k$ | measure of variation, defined in Ch. V |
| $\Omega(\lambda_k)$ | function used for determining convergence zone spacing, defined in Ch. VII |

$\Omega_{k,\infty}$ limiting value of $\Omega$

$\omega_R(r)$, $\hat{\omega}_R(r)$ } weighting functions

Notes

1. A metric is a generalization of the concept of distance. It is a function of two elements of the space (in this case transmission loss curves) into the nonnegative real numbers. A number of metrics exist for function spaces, but it is extremely difficult to give a meaning to the metric, as it applies to transmission loss curves.

2. The problem of comparing a number of transmission loss curves is not significantly different from that of comparing two such curves. One may compare the curves pairwise and then form composite measures from all possible pairs. Or one may select one curve as the 'base curve' and compare all other curves to it. The details of the multiple curve comparisons will not be addressed in this paper.

3. The need for an automated procedure precludes having an acoustician within the processing loop making somewhat subjective judgements. But this in no way implies that the judgment of the analyst is not needed. Critical evaluation of the results by the analyst is a requirement, and these measures serve as a tool to indicate what the types of differences are, and how great they are. But these measures will not, by themselves, ever explain why a particular characteristic is present or absent. The requirement for reasonably efficient methods of computation rule out some of the more esoteric methods of pattern recognition.

4. The problem of comparing two transmission loss fields is not addressed to this paper. If the two fields were grids whose set of depths matched, then one could compare the fields by comparing the two transmission loss curves at each common depth.

5. To circumvent this problem, it will be assumed throughout this paper that the transmission loss curve is a linear spline whose grid points are the tabulated values of the transmission loss. In other words, the transmission loss curve is obtained from the transmission loss points by 'connecting the dots'. More sophisticated interpolatory techniques could be utilized in place of straight line segments, but the advantage appears to be minimal and the resulting complexity (in both interpolation and quadrature) is substantial.

6. i.e., for any r in the interval [a,b] both $T_1(r)$ and $T_2(r)$ will be defined.

7. $L_p$ forms a norm only for $p \geq 1$, but the form (and the function space) is defined for any $p > 0$. For p between 0 and 1 the $L_p$ space is not a Banach space. Note that $L_2$ and $L_\infty$ correspond to standard deviation and maximum deviation, which form the basic measures of perturbation.

8. Thus, any concept of 'closeness' for transmission loss curves must take into account the phenomena of shifting caustics such as in Figure 1.

9. A point criteria is any sort of measure or functional which depends on examining the functions $T_k(r)$ at fixed range points, rather than viewing them as elements of a function space. Since the $L_p$ norms measure differences in the $T_k(r)$ at various points (albeit an infinite number of points), they are essentially point criteria.

10. Obviously the range to which a transmission loss function is known is a major concern, and if it is too short the true nature of the curve may not be apparant. But a scheme of analysis must not be so unstable that the results are highly dependent upon whether the transmission loss data cuts off at a convergence zone or a shadow zone.

11. If one is dealing with shallow water propagation, RAP propagation, etc., then these numbers are not applicable; others may be substituted.

12. This is an example (albeit somewhat detailed) of the reasoning which led to the empirical values of many parameters and functions in this paper. Refinement of such estimates based on a large number of curves is necessary prior to operational use of the measures generated in this paper.

13. This, of course, is frequency dependent.

14. If the two curves are at different frequencies, there is considerable latitude in the choice of the attenuation coefficient $\alpha$ for this curve. It appears that the geometric mean of the two individual attenuation coefficients is a reasonable value.

15. These fluctuations may be due to actual phenomena, model characteristics, or measurement error.

16. In this step we know that

$$\tilde{\kappa}^2 \leq \Theta_1(\ell_1) < \kappa^2$$

so that there is some variation between $T_1$ and $\ell_1$. Consider three possible forms for $T_1(r)$ whose perturbation function $P_1(r)$ appear as the three curves in Figure 21. Assume $\Theta_1(\ell_1)$ is the same for each of the three $T_1$, so that the three curves $P_1(r)$ have the same geometric second weighted moments. (The geometric second moment of $P_1(r)$ with weight $f(r)$ is $\Theta_1(\ell_1)$.) In Figure 21a the data shows fluctuations of period less than $\tilde{p}$, such as could be produced from a coherent summation model. In this case, $\chi_1$ will be the variation from 'top to bottom' of a cycle and $\sigma_1$ will be rather small compared to $\tilde{p}$. In Figure 21b, we still have significant variation

with a distance $\tilde{p}$, but $\sigma_1$ will now be close to $\tilde{p}$. This behavior (with period of a few $\tilde{p}$) represents actual convergence zones, where one can drop from caustic to shadow within distance $\tilde{p}$. In Figure 21c, we see behavior of a period much greater than $\tilde{p}$, and far too large to be convergence tones. This sort of behavior could occur when a propagation loss curve is almost monotonic, but is essentially 20 log r for the first several miles, then 10 log r, then changes due to the crossing of a front, or a rise in the ocean bottom. A single logarithmic component $\ell_1$ cannot match the three different types of behavior, so a slowly-varying function is produced for $P_1$. In this case, $\chi_1$ will be rather small in comparison with $\sqrt{\Theta_1(\ell_1)}$. This is the rationale behind the choice of tests in the second step of the convergence zone determination.

17. To summarize this three step test, the logic is given in Figure 22.

18. Particularly those with coherent phase summation.

19. This is equivalent to smoothing the transmission loss function.

20. It is inadequate to simply search for the maximum, for that could occur at range $\delta$, such as in Figure 11.

21. This can occur when the second derivative changes so as to indicate a perturbation from the logarithmic component. In such a case $\Phi_k(R)$ will have a local maximum, but $T_k(R)$ will not.

22. The restriction to positive $\lambda$ should be obvious: the summation diverges when $\lambda = 0$.

23. As before, the use of f(r) as a weighting function is to decrease the sensitivity of $\Omega$ to $r_k$.

Figure 21. Perturbation function for three cases, relative to distance $\tilde{p}$

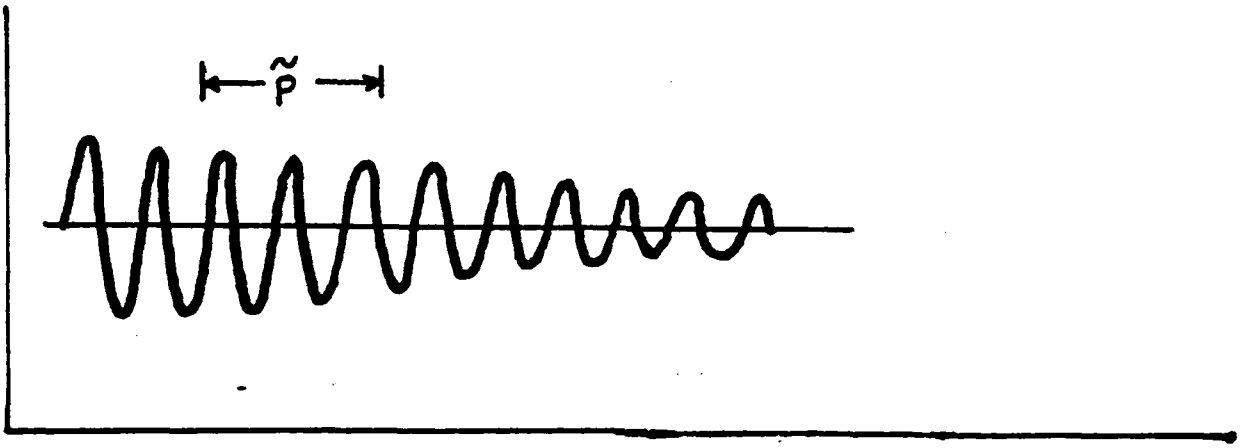


a) High total variation of curve, indicating scatter

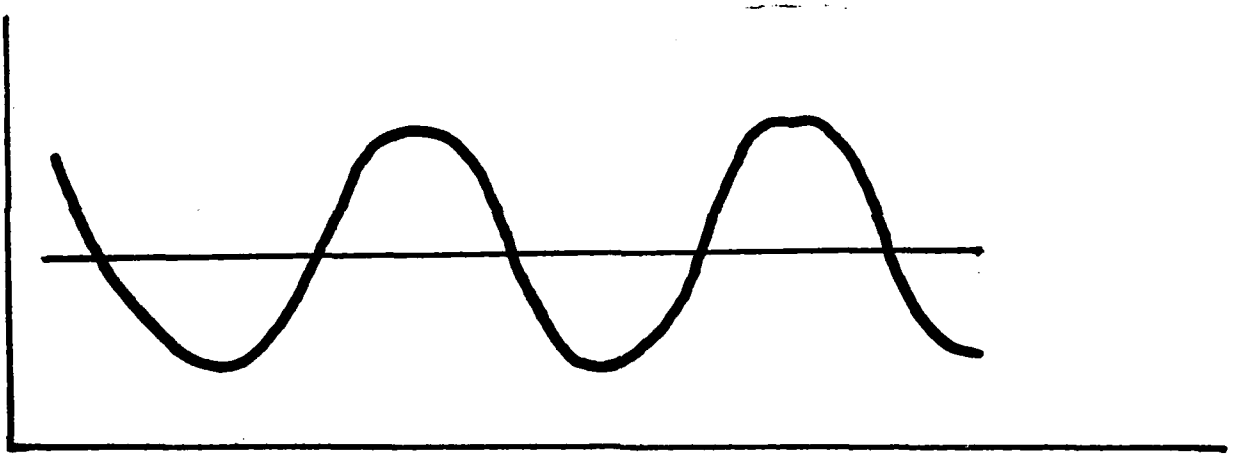

b) Smaller total variation of curve, indicating convergence zones

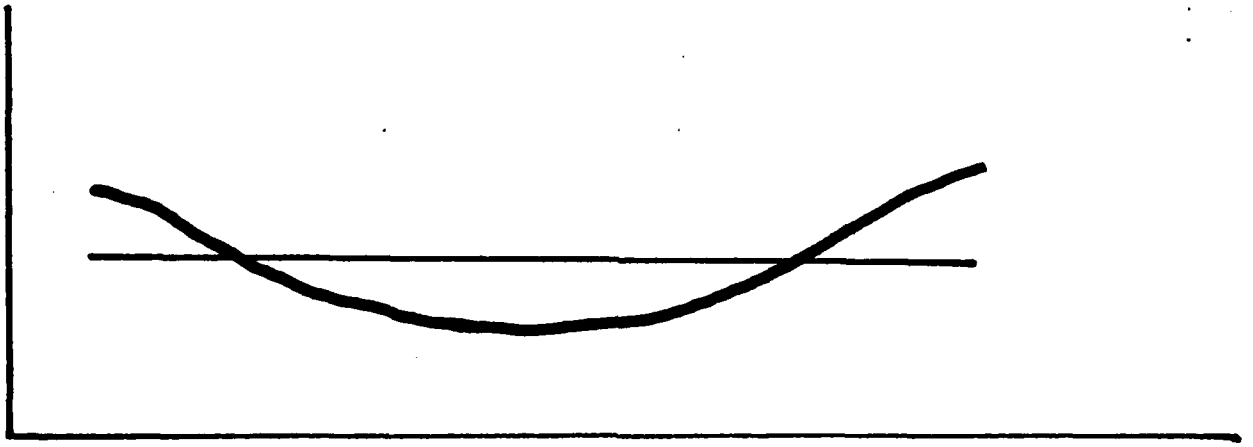

c) Slowly varying function, indicating no convergence zones

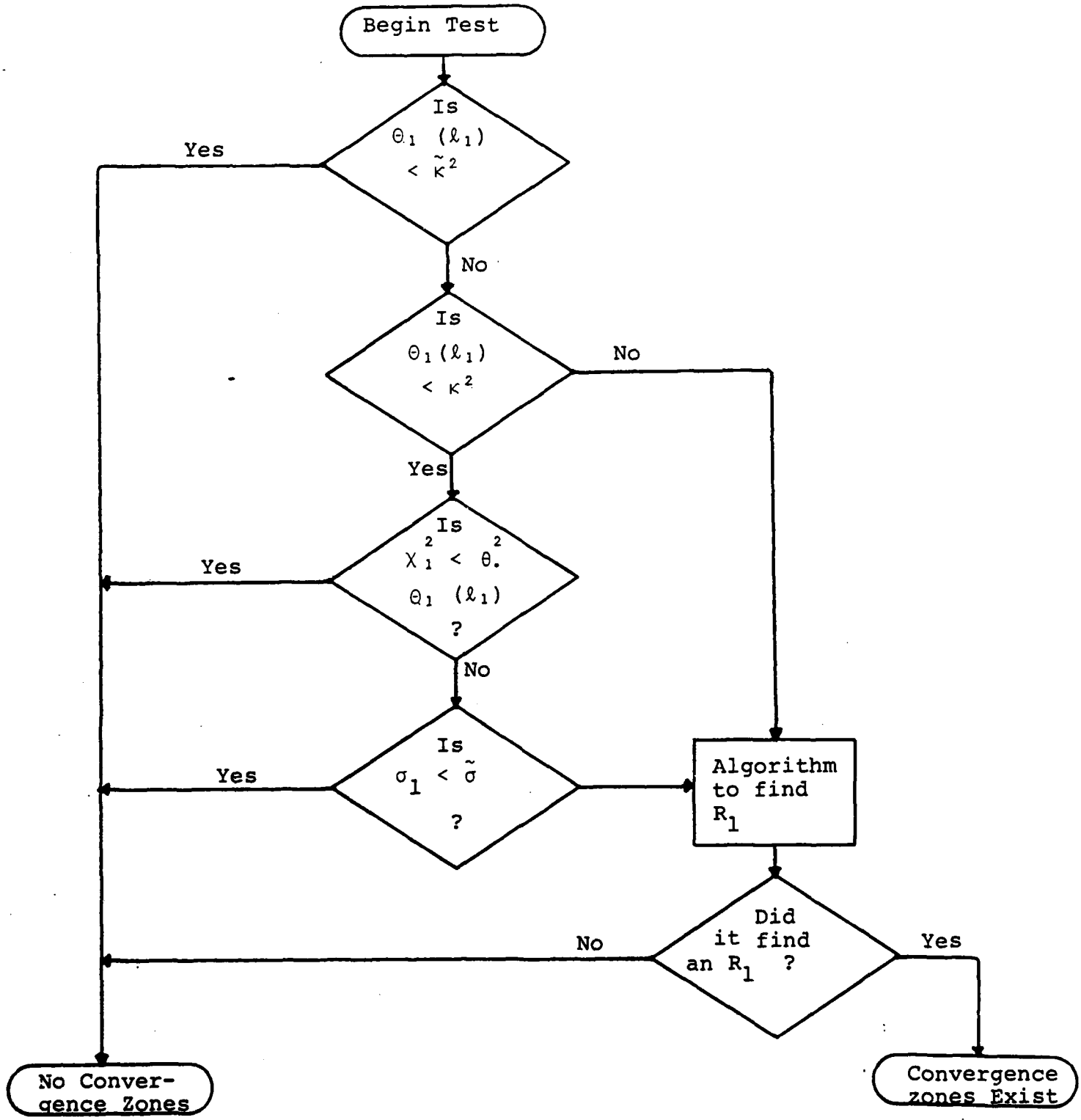


Figure 22 Logic of Three-Step Test

24. Although $Q_{\lambda_k}(r)$ is given by an infinite series, there are at most

$$\frac{\varepsilon+r_k-R_1}{\lambda_k}+1$$

terms which are not identically zero on the interval $[\delta,r_k]$. Thus, the evaluation of $\Omega(\lambda_k)$ may be done using a finite number of terms.

25. The function $\Omega(\lambda_k)$ is $C^1$.

26. If one formally expresses $\Omega(0)$ the indeterminate form $\infty/\infty$ leads one to believe that $\Omega(0)$ should have the value $\Omega_k,\infty$. However, this is not the limit of $\Omega(\lambda_k)$ as $\lambda_k$ decreases to 0.

27. Since the domain of $\lambda_k$ is the open interval $(0,\infty)$ a maximum need not exist for $\Omega(\lambda_k)$. But this function is constant for large $\lambda$ and has a limit for small $\lambda$, hence the supremum, which always exists, is either the maximum (if it exists) or the limit, i.e.

$$\sup \Omega(\lambda_k) = \begin{cases} \max \Omega(\lambda_k) & \text{if it exists} \\ \lim_{\lambda_k \downarrow 0} \Omega(\lambda_k) & \text{if max does not exist} \end{cases} .$$

Of course, whenever this limit is less than $\Omega_k,\infty$ the maximum exists.

28. If the maximum peak of $P_k$ (as opposed to $T_k$) occurs at $R_1$, then it is obvious that

$$\Omega(\lambda_k) \leq \Omega_k,\infty \quad \text{for } \lambda_k>0$$

and

$$\Omega(\lambda_k) < \Omega_k,\infty \quad \text{for } \lambda_k<r_k+\varepsilon-R_1 \quad .$$

29. The desired maximum is

$$\lambda_k = R_2 - R_1$$

whereas the true maximum occurs for any

$$\lambda_k \geq r_k + \varepsilon - R_1$$

and since one can only talk about a second convergence zone range $R_2$ if $R_2$ is less than $r_k$, one has

$$\lambda_k \geq r_k + \varepsilon - R_1 > R_2 + \varepsilon - R_1 > R_2 - R_1$$

Therefore, the true maximum cannot be the desired maximum.

30. Even if the maximum peak of $P_k$ is not at $R_1$ (as in Figure 13) but elsewhere, trouble can develop. In Figure 14 the true maximum of $\Omega(\lambda_k)$ will occur at

$$\lambda_k = R_3 - R_1$$

whereas the desired local maximum is at

$$\lambda_k = R_2 - R_1 \quad .$$

31. I.e. the interval should not contain both $R_1$ and $R_3$ in Figure 14.

32. Which, of course, is a geometric attribute and is usually described qualitatively.

33. If $\delta/r_{12}$ is small enough (e.g., less than 1/8) then if the curves are close their coefficients should be close as well, provided that the attenuation coefficient $\alpha$ is the same for both $\ell_k$. If $\delta/r_{12}$ is large (e.g. 1/2) or the two curves $T_k$ are for different frequencies (so that the attenuation coefficients differ) then it is quite common to have the $\ell_k$ curves relatively close over $[\delta, r_{12}]$, but have the coefficients $b_k, \hat{b}_k$ vastly different.

34. There is always the possibility that one curve has measure just below the threshold $\kappa^2$, the other has measure just above the threshold, and the two curves are quite close but the

indicator $T_\beta$ is 1. This is a problem of binary decisions in general. The decision as to the existance convergence zones (cf. Fig. 22) is a binary choice, even though transmission loss curves may vary continuously from a no convergence zone situation to existance of convergence zones.

35. One may also devise measures based on $\chi_k$, such as

$$\chi_1 - \chi_2$$

or

$$\frac{\chi_1}{\chi_2} \sqrt{\frac{\Theta_2(\ell_2)}{\Theta_1(\ell_1)}}$$

provided $\chi_2$ is not zero. But at this time it appears that the measures $T_\gamma$ and $T_\zeta$ will be adequate.

36. See note 2.

37. Though they usually will have a peak every $\lambda_k$ or so.

38. See note 5.

39. The first minor is obtained by multiplying $(-1)^{i+j}$ by the determinant obtained by deleting the $i^{th}$ row and $j^{th}$ column of the determinant A(k).

40. These second minors are obtained by multiplying $(-1)^{i+j+m+n}$ by the determinant obtained by deleting the $i^{th}$ and $j^{th}$ rows and $m^{th}$ and $n^{th}$ columns of A(k).

41. The reason for ignoring the reflected paths is the simplification of the analysis. It is possible to do the analysis with surface and bottom reflected rays, but then the field would not be represented as easily. The family of ray paths would consist not simply of the one set of analytic functions, but would be a countable set of piecewise analytic functions.

42. In this case

$$\zeta = \frac{\partial z}{\partial \theta_1} = \frac{\partial z}{\partial \theta_o} \frac{d\theta_o}{d\theta_1} \quad .$$

43. If it were zero the raypath would not pass through the source since $z_1 \neq z_o$.

44. As a result of that, one may easily obtain branches which are false roots. More serious for numerical work, however is the problem of identification of branches, since a single value of $\xi$ will produce eight pairs (x,y) of points (not all of which need be real).

## REFERENCES


a. Karl Friedrich Gauss: "Theoria motus corporum coelestium in sectionibus conicis solem ambientium", 1809.

b. Karl Friedrich Gauss: "Theoria combinations observationum erroribus minimus obnoxiae", 1823.

c. Clive B. Moler and L. P. Solomon: "Use of Splines and Numerical Integration in Geometric Acoustics", JASA, Vol. 48 (1970).

d. Louis P. Solomon and L. Armijo: "An Intensity Differential Equation in Ray Acoustics", JASA, Vol. 50 (1971).

e. Julian L. Coolidge: "A Treatise on Algebraic Plane Curves", 1929.

thresholds for tests dealing with existance of convergence zones, used in Ch. VI